31183-6001-RU-00
CR-152183

(NASA-CR-152183) EXTENDED DEVELOPMENT OF VARIABLE CONDUCTANCE HEAT PIPES Final Report (TRW Defense and Space Systems Group) 56 p HC A04/MF A01 CSCL 20D
N78-33379
Unclas
G3/34 32154

EXTENDED DEVELOPMENT OF VARIABLE CONDUCTANCE HEAT PIPES

CONTRACT NAS 2-9834

FINAL REPORT

SEPT 1978

Prepared for

NASA AMES RESEARCH CENTER

MOFFET FIELD, CALIF, 94035

TRW SALES NO. 31183.000

TRW
DEFENSE AND SPACE SYSTEMS GROUP

ONE SPACE PARK • REDONDO BEACH • CALIFORNIA

EXTENDED DEVELOPMENT OF VARIABLE CONDUCTANCE HEAT PIPES

FINAL REPORT
SEPTEMBER 1978
CONTRACT NAS 2-9834

D. Antoniuk
D.K. Edwards
E.E. Luedke

Prepared for
NASA AMES RESEARCH CENTER
MOFFET FIELD, CALIF, 94035

TRW SALES NO. 31183.000

TRW
DEFENSE AND SPACE SYSTEMS GROUP
ONE SPACE PARK • REDONDO BEACH, CALIFORNIA 90278

CONTENTS

		Page
1.	INTRODUCTION	1
2.	FURTHER RESEARCH ON THE VAPOR MODULATED HEAT PIPE (VMHP)	2
2.1	Design	2
2.2	Experimental Investigation of Transient Response of (VMGP)	2
2.2.1	Test Procedure	2
2.2.2	Test Parameters	5
2.2.3	Test Results	6
2.3	Investigation of the Use of Non-Condensible Gas	15
2.3.1	Theoretical Analysis	15
2.3.2	Experimental Results	15
2.4	Theoretical Investigation of Transient Response	18
2.4.1	Discussion	18
2.4.2	Mathematical Model Elements	20
2.4.3	Computer Program Elements and Organization	26
2.4.4	Results and Conclusions	28
3.	DEVELOPMENT OF VAPOR INDUCED DRYOUT DIODE HEAT PIPE	29
3.1	Introduction	29
3.2	Basic Operating Principle	30
3.3	Design of Diode Heat Pipe	30
3.3.1	The Valve Bulkhead Design	32
3.3.2	The Wick Feed-Thru	32
3.3.3	Reed Valve Assembly Tests	34
3.3.4	Heat Pipe Diode Test Results	35
3.4	Conclusions	37
APPENDICES		
A		39
B		48

1.0 INTRODUCTION

TRW has been actively involved during the last few years in the development of variable conductance heat pipes for application in advanced space thermal control systems. In 1975, under Contract NAS2-8310 to Ames Research Center, TRW fabricated and tested two prototype vapor-modulated heat pipes which achieved variable conductance by induced wick/groove dry-out. The first prototype was designed for moderate capacity in a double-heat-pipe configuration. Tests of this prototype showed the roundness of the new induced-dry-out mechanism and uncovered some secondary elements that adversely affected performance. Recommendations for an improved design were subsequently incorporated in the fabrication of a second high-capacity vapor-modulated prototype. The new design, which uses a short vapor-modulated heat pipe to couple two conventional heat pipes, was tested successfully. The heat pipe operated at twice the 100-watt design heat load, and the source temperature was practically independent of sink conditions and increased with heat load at a rate of only 0.03°C per watt. The results of the preliminary tests, as well as details of the configuration of the heat pipe, are presented in a research report, CR-137782, prepared for Ames Research Center.

In 1977, under Contract NAS 2-9834, TRW undertook a program to use the aforementioned high-capacity vapor-modulated heat pipe to study protection from freezing-point failure, increased control sensitivity, and transient behavior under a wide range of operating conditions in order to determine the full performance potential of the vapor-modulated heat pipe. In addition, a new concept, based on the vapor-induced-dry-out principle, was developed for passive feed back temperature control as a heat pipe diode.

This report documents the work performed under the contract and describes a) the experimental and theoretical investigation of the performance of the vapor-modulated heat pipe, and b) the design, fabrication and test of the heat pipe diode.

2.0 FURTHER RESEARCH ON THE VAPOR MODULATED HEAT PIPE (VMHP).

2.1 Design.

The details of the VMHP are presented in Research Report CR-137782, prepared for Ames Research Center. However, for completeness, certain basic design features of the heat pipe are briefly described in what follows. The high-capacity design has a triple-heat-pipe configuration. The tested configuration is shown in Figure 2.1(c). Two conventional 1.27-cm OD, uniform porosity metal fiber slab wick heat pipes are coupled by a 2.54-cm OD vapor modulated heat pipe 15.2-cm long. The coupler heat pipe uses a wick assembly with a two-step gradation in porosity. The wick porosity on the condenser side of the bulkhead, which supports the bellows/valve assembly, is 86%, and on the evaporator side is 76%. Ammonia is the working fluid in all three heat pipes. The bellows and sensor volumes are filled with perflamopentane.

2.2 Experimental Investigation of Transient Response of VMHP.

2.2.1 Test Procedure.

The heat pipe was instrumented with eighteen copper-constantan thermocouples located along the pipe as shown in SK 75061 in Appendix A. All the temperatures, except TC 7, were monitored with a 24-channel strip chart recorder. Owing to the rather slow response of this instrument (1.5 to 2 minutes printing interval), a fast response single-pen millivolt strip chart recorder was used to continuously monitor the transient behavior of the input heat pipe adiabatic temperature, TC 7. Certain features of this instrument, such as its adjustable zero and variable span, were necessary in order to observe with high resolution the details of the temperature response profiles that would enable a better understanding of the characteristics of the vapor-induced dry out mechanism. A sample temperature profile recorded with this instrument during one of the test runs is shown in Figure 2.2.

Two heat source configurations were used to simulate variations in the thermal mass of the evaporator section. A 1.3 Kg aluminum block with tape heaters attached to it, and the sensor inserted into a hole drilled into it, was used for the high thermal mass simulation. To simulate a thermal resistance

ORIGINAL PAGE IS
OF POOR QUALITY

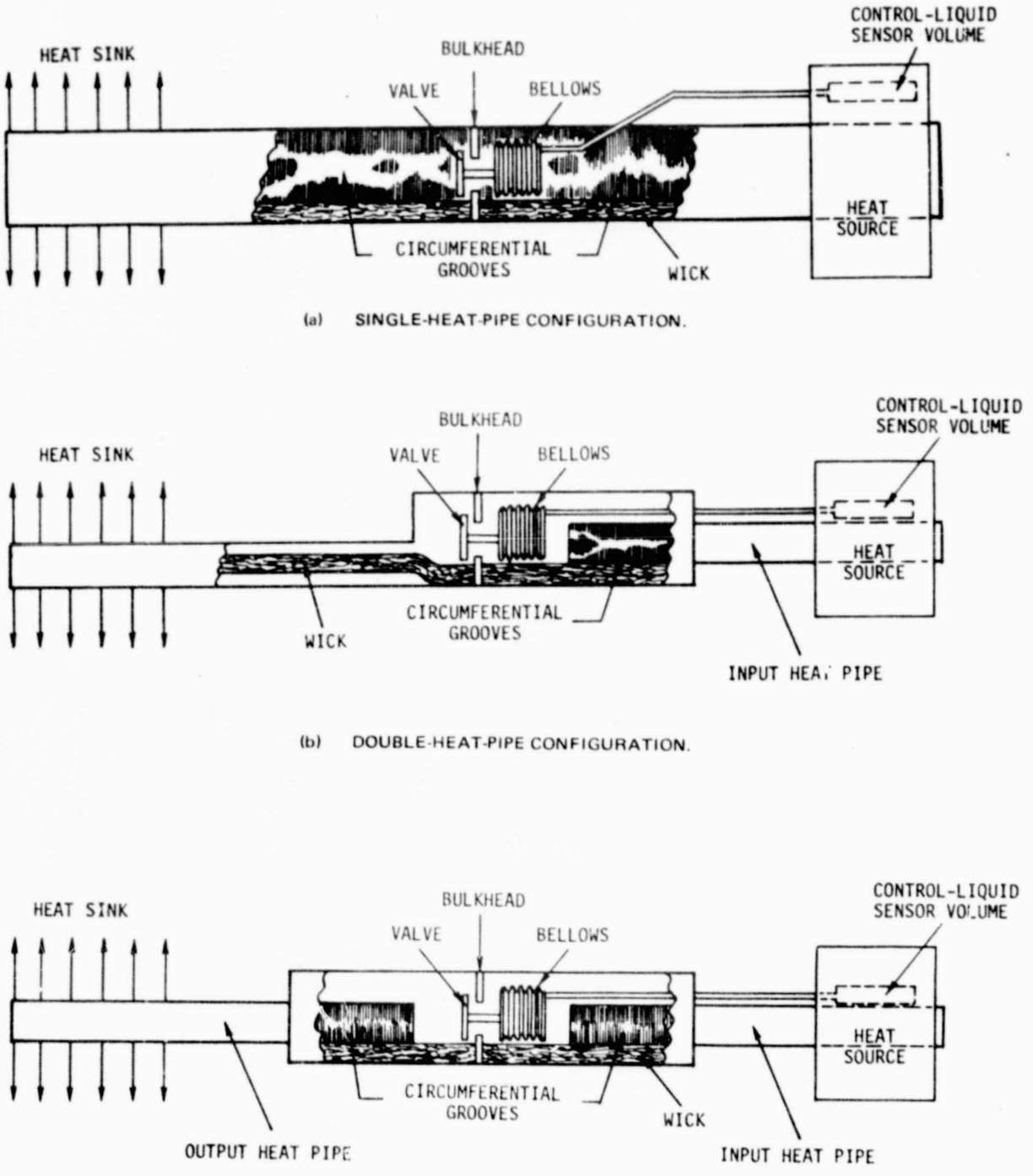

Figure 2.1. Vapor Modulated Heat Pipe Based on Induced Wick/Groove Dry Out

ORIGINAL PAGE IS
OF POOR QUALITY

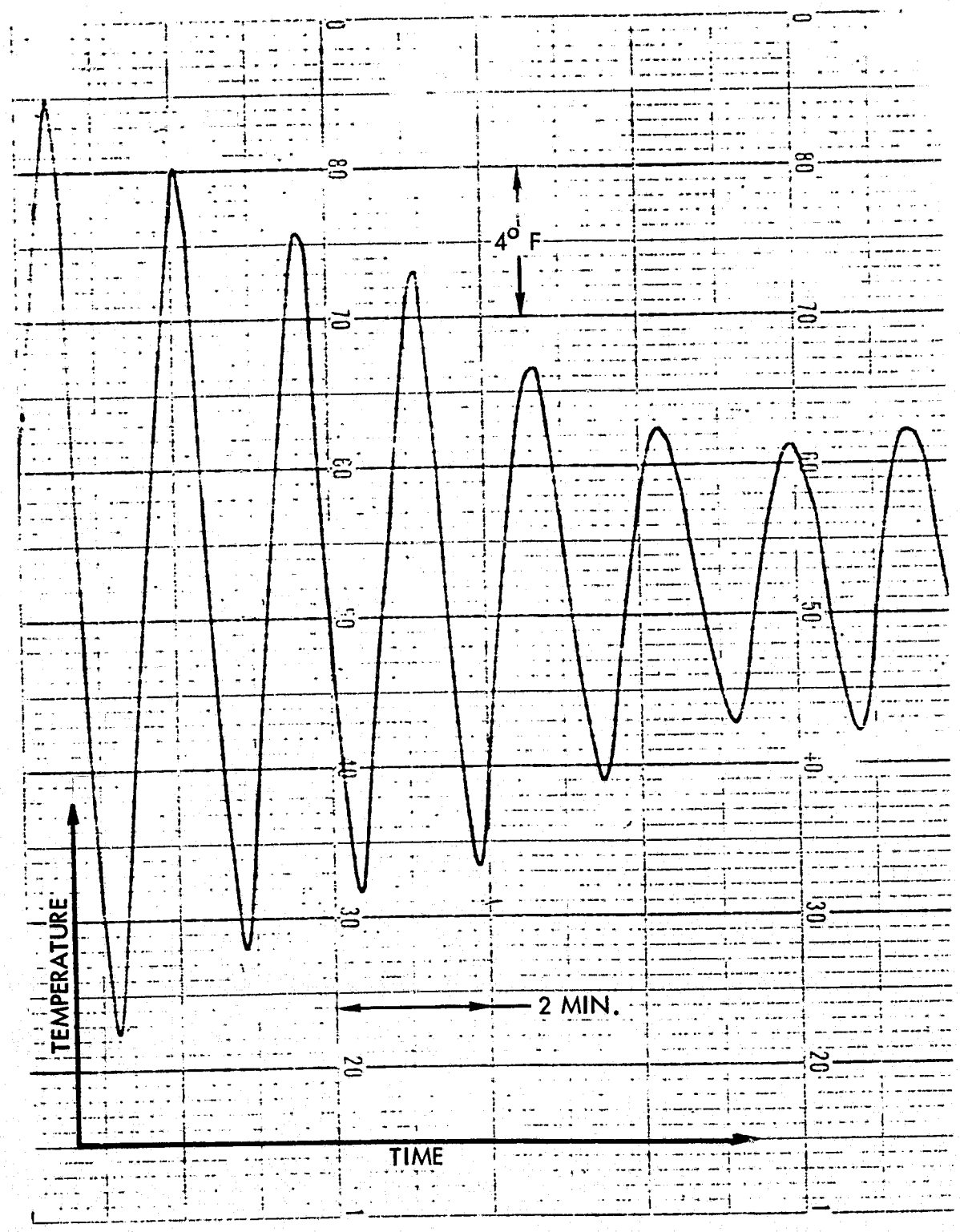

Figure 2.2. Sample Transient Temperature Profile of VMHP as Recorded with Fast-response Instrument

between a heat pipe and the equipment whose temperature is being controlled, .006 inch of Teflon was placed between the heater block and the evaporator saddle.

For the low thermal mass simulation, the aluminum block was removed, and the tape heaters were placed directly on top of the evaporator saddle. The sensor was inserted into a copper flange and mounted on the saddle between the tape heaters. The copper flange was designed to provide a nearly uniform temperature distribution around the perimeter of the sensor tube. The thermal resistance between the source and the heat pipe resulted from .006 inch of Teflon placed between the heat pipe and the evaporator saddle.

The condenser section of the output heat pipe was clamped between two 0.5-inch thick aluminum saddles and mounted on a temperature-controlled cold plate. To simulate a conderser thermally close-coupled to a sink, a thin film of RTV was placed between the condenser saddle and the cold plate. The operation of the heat pipe in space was simulated by inserting 3/16 inch of Teflon between the condenser saddle and the cold plate.

2.2.2 Test Parameters.

Several operating parameters such as the source thermal mass, condenser thermal resistance, sink temperature, sensor volume and power input were varied to determine their effects on the transient behavior of the vapor modulated heat pipe. The range of these parameters is shown in Table 2.1

Table 2.1. Range of Test Parameters

Evaporator Block Mass (M)	.13 - 1.3 Kg
Control Sensor Volume (V)	2.45 - 4.90 cc
Input Power	0 - 100 watts
Condenser Section Thermal Resistance (R)	.10 - .63 ^{o}C/watt
Sink Temperature	-57 - -18 ^{o}C

2.2.3 Test Results.

The results from forty-two test runs are summarized in Table 2.2. Selected transient profiles of the input heat pipe adiabatic temperature are shown in Figures 2.3 through 2.8. The salient effects of the operating parameters on the performance of the heat pipe are discussed below.

2.2.3.1 The Source Mass.

As expected, the thermal mass of the heat source was the most important parameter that determined whether the heat pipe operates in a stable or unstable mode. All high mass runs were unconditionally stable and generally characterized by a single damped temperature oscillation after a step change in power followed by stable operation. On the other hand, low mass runs were found to be characterized in general by temperature oscillations whose amplitude and frequency depended to various degrees on other operating parameters.

2.2.3.2 The Sink Temperature.

Under stable operating conditions, the sink temperature has a relatively minor effect, namely a shift in the operating temperature level of the heat pipe and the source. This effect can be seen in Figures 2.3 and 2.4, where the input heat pipe adiabatic temperature is shown as the power is increased in steps from 0 to 100 watts for sink conditions of -75°F and 0°F, respectively. The transient profiles are seen to be quite similar, except that the overall temperature level is 2°F to 4°F higher at 0°F sink than at -75°F sink.

For runs where temperature oscillations were present, lower sink temperatures had a stabilizing effect. This can be seen in Figures 2.5, 2.6 and 2.7 which show the adiabatic temperature of the input heat pipe of the VMHP operated at 100 watts with a small source mass, large sensor, and the condenser close-coupled to the sink which was held at temperatures of 0°F, -35°F, and -70°F, respectively. Large temperature oscillations at 0°F are substantially reduced and eventually completely damped as the sink dropped to -35°F and -70°F, respectively. For the lowest sink condition, the onset of temperature oscillations after a period of stable operation can be attributed to an observed drift upward of the sink temperature. This observation would seem to indicate that the oscillations were critically damped near a sink temperature of -70°F, and that further lowering of the sink temperature could have resulted in continuous stable operation at 100 watts.

FOLDOUT FRAME 1

ORIGINAL PAGE IS
OF POOR QUALITY

Run No.	Power Input (Watts)	Sink Temperatures (°F)	Condenser Thermal Resistance	Evaporator Block Mass	Sensor Volume	Input Heat Pipe Adiabatic Section				
						Maximum Temp., °F	Minimum Temp., °F	Period Minutes	Mean or S.S. Temp., °F	
1	50	-70°	.63°C/Watt	1.3 Kg	2.45 cc	NA*	NA*	NA*	79	86
2	75	↓	↓	↓	↓	NA	NA	NA	82	88
3	100	↓	↓	↓	↓	NA	NA	NA	75	
4	50	-35°	↓	↓	↓	90	80	1.4(HalfPeriod)	82	
5	75	↓	↓	↓	↓	NA	NA	NA	82	
6	100	↓	↓	↓	↓	78.5	78	Variable	--	
7	50	-70°	.1°C/Watt	↓	↓	NA	NA	NA	80	
8	75	↓	↓	↓	↓	NA	NA	NA	78	
9	100	↓	↓	↓	↓	NA	NA	NA	75	
10	50	-35°	↓	↓	↓	NA	NA	NA	84	
11	75	↓	↓	↓	↓	NA	NA	NA	80	
12	100	↓	↓	↓	↓	NA	NA	NA	78	
13	50	0°	↓	↓	↓	92	81	1.4(HalfPeriod)	83	
14	75	↓	↓	↓	↓	NA	NA	NA	82	
15	100	↓	↓	↓	↓	NA	NA	NA	78	
16	50	-70°	↓	.13 Kg	↓	74	54	1.0(HalfPeriod)	60	
17	75	↓	↓	↓	↓	62	59	1.4 "	64	
18	100	↓	↓	↓	↓	65	52	2.4	58	
19	50	-35°	↓	↓	↓	77	61	1.8	69	
20	75	↓	↓	↓	↓	74	50	1.5	62	
21	100	↓	↓	↓	↓	69	45	1.4	57	
22	50	0°	↓	↓	↓	77	59	1.7	68	
23	75	↓	↓	↓	↓	74	54	1.7	69	
24	100	↓	↓	↓	↓	69	48	1.6	58	
25	50	-70°	.1°C/Watt	↓	4.9 cc	77	47	2.4(.6↓,1.8↑)	62	
26	75	↓	↓	↓	↓	69	29	2.1	49	
27	100	↓	↓	↓	↓	52	17	1.8	35	
28	50	-35°	↓	↓	↓	97	77	2.0	87	
29	75	↓	↓	↓	↓	97	45	2.4	71	
30	100	↓	↓	↓	↓	{85 69}	{38 68}	{1.9 2.5}	{62 68}	
31	50	0°	↓	↓	↓	104	82	2.2	83	
32	75	↓	↓	↓	↓	99	64	2.2	82	
33	100	↓	↓	↓	↓	95	58	2.1	77	
34	50	-70°	↓	1.3 Kg	↓	NA	NA	NA	104	
35	75	↓	↓	↓	↓	NA	NA	NA	108	
36	100	↓	↓	↓	↓	NA	NA	NA	112	
37	50	-35°	↓	↓	↓	NA	NA	NA	126	
38	85	↓	↓	↓	↓	NA	NA	NA	129	
39	100	↓	↓	↓	↓	NA	NA	NA	126	
40	50	0°	↓	↓	↓	NA	NA	NA	138	
41	75	↓	↓	↓	↓	NA	NA	NA	136	
42	100	↓	↓	↓	↓	NA	NA	NA	135	

*NA = Not Applicable

ORIGINAL PAGE IS
OF POOR QUALITY

FOLDOUT FRAME 2

TABLE 2-2. VAPOR MODULATED TRANSIENT TEST RUNS

rator ck s	Sensor Volume	Input Heat Pipe Adiabatic Section Maximum Temp., °F	Minimum Temp., °F	Period Minutes	Mean or S.S. Temp., °F	Initial Overshoot, °F	Remarks
Kg	2.45 cc	NA*	NA*	NA*	79	86.5-79 = 7.5	No oscillations.
		NA	NA	NA	82	88.5-82 = 6.5	No oscillations.
		NA	NA	NA	75	80-75 = 5	No oscill..Overshoot from 50 watts.
		90	80	1.4(HalfPeriod)	82	---	Single Damped oscillation.
		NA	NA	NA	82	---	No oscillations.
		78.5	78	Variable	--	---	Irregular oscillations, then burn out.
		NA	NA	NA	80	87-80 = 7	No oscillations.
		NA	NA	NA	78	80-78 = 2	No oscillations. Overshoot from 50 watts.
		NA	NA	NA	75	78-75 = 3	No oscillations. Overshoot from 75 watts.
		NA	NA	NA	84	92-84 = 8	No oscillations.
		NA	NA	NA	80	84-80 = 4	No oscillations. Overshoot from 50 watts.
		NA	NA	NA	78	81-78 = 3	No oscillations. Overshoot from 75 watts.
		92	81	1.4(HalfPeriod)	83	---	Single damped oscillation.
		NA	NA	NA	82	84-82 = 2	No oscillations. Voershoot from 50 watts
		NA	NA	NA	78	81-78 = 3	No oscillations. Overshoot from 75 watts.
Kg		74	54	1.0(HalfPeriod)	60	---	Single damped oscillation.
		62	59	1.4 "	64	---	Single damped oscillation.
		65	52	2.4	58	---	Intermittent damped oscillation.
		77	61	1.8	69	84-69 = 15	Steady oscillations.
		74	50	1.5	62	---	Steady oscillations.
		69	45	1.4	57	71-57 = 14	Steady oscillations. Overshoot from 75 watts.
		77	59	1.7	68	83-68 = 15	Steady oscillations.
		74	54	1.7	69	---	Variable amplitude oscillations.
		69	48	1.6	58	---	Variable amplitude oscillations.
	4.9 cc	77	47	2.4(.6↓,1.8↑)	62	85-62 = 23	Irregular amplitude oscillations.
		69	29	2.1	49	71-49 = 22	Steady oscillations. Overshoot from 50 watts.
		52	17	1.8	35	53-35 = 28	Intermittent stable oscill. Overshoot from 75 watts
		97	77	2.0	87	108-87 = 21	Steady oscillations.
		97	45	2.4	71	---	Steady oscillations.
		{85 69}	{38 68}	{1.9 2.5}	{62 68}	---	{Initial damped oscillations. Residual steady oscillations.}
		104	82	2.2	83	118-83 = 35	Steady oscillations.
		99	64	2.2	82	---	Steady oscillations.
		95	58	2.1	77	---	Steady oscillations.
Kg		NA	NA	NA	104	111-104 = 7	No oscillations.
		NA	NA	NA	108	---	No oscillations.
		NA	NA	NA	112	---	No oscillations.
		NA	NA	NA	126	128-126 = 2	No oscillations.
		NA	NA	NA	129	---	No oscillations.
		NA	NA	NA	126	---	No oscillations.
		NA	NA	NA	138	144-138 = 6	No oscillations.
		NA	NA	NA	136	---	No oscillations.
		NA	NA	NA	135	---	No oscillations.

*NA = Not Applicable

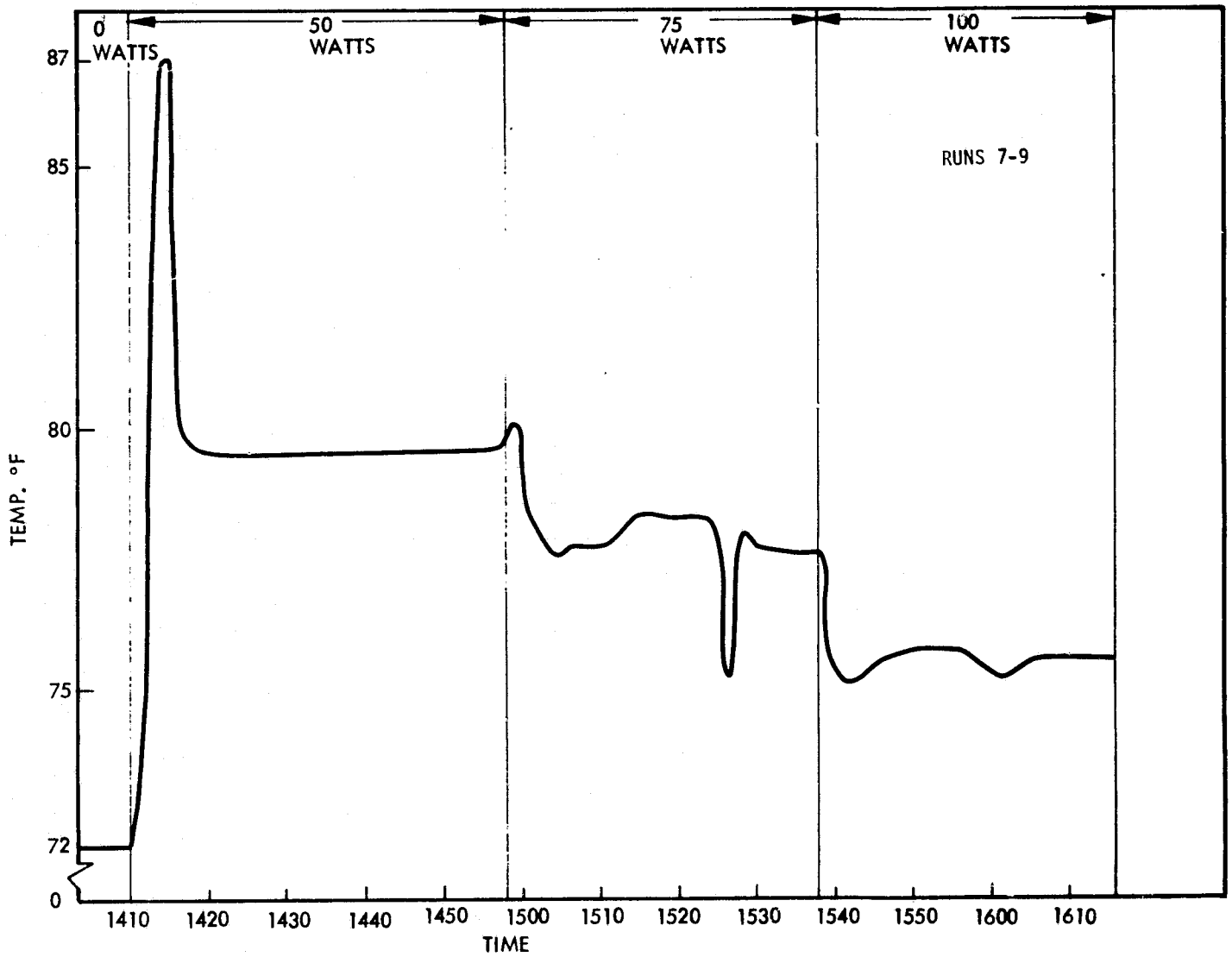

Figure 2.3. Effect of Power on Input Heat Pipe Adiabatic Temperature for -70°F Sink

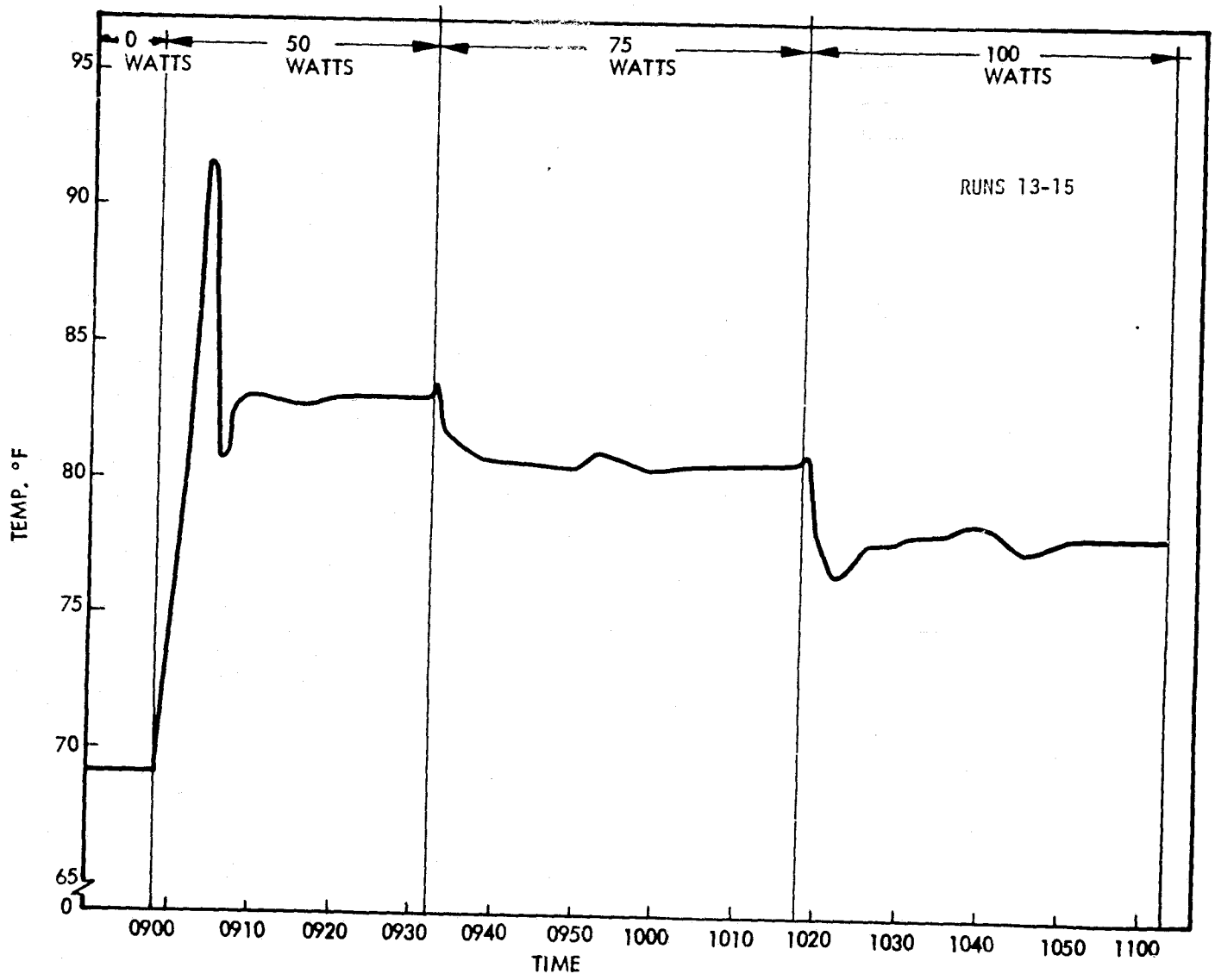

Figure 2.4. Effect of Power on Input Heat Pipe Adiabatic Temperature for $0^{o}F$ Sink

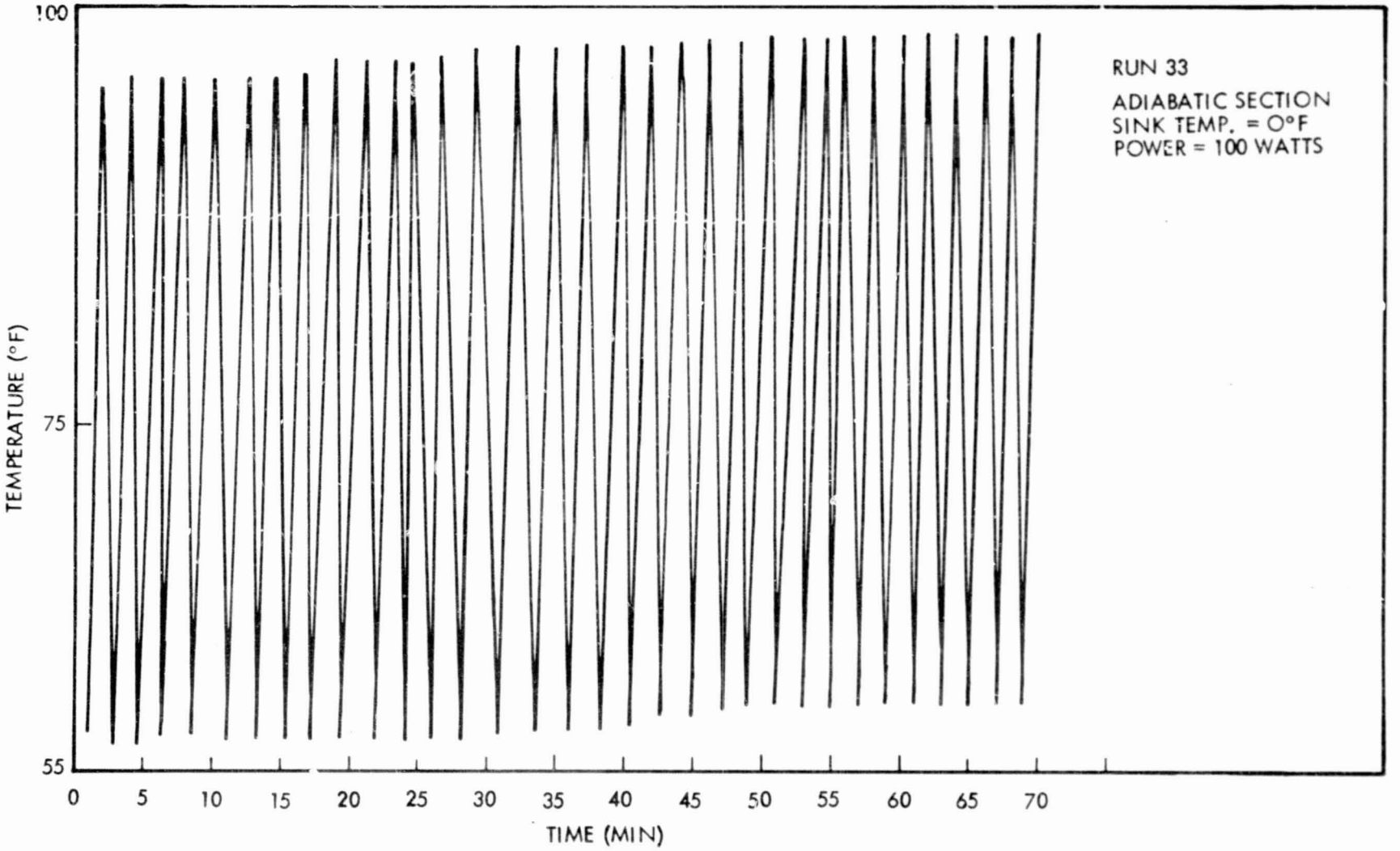

Figure 2.5. Transient Response of Input Heat Pipe for 0^{o}F Sink

ORIGINAL PAGE IS
OF POOR QUALITY

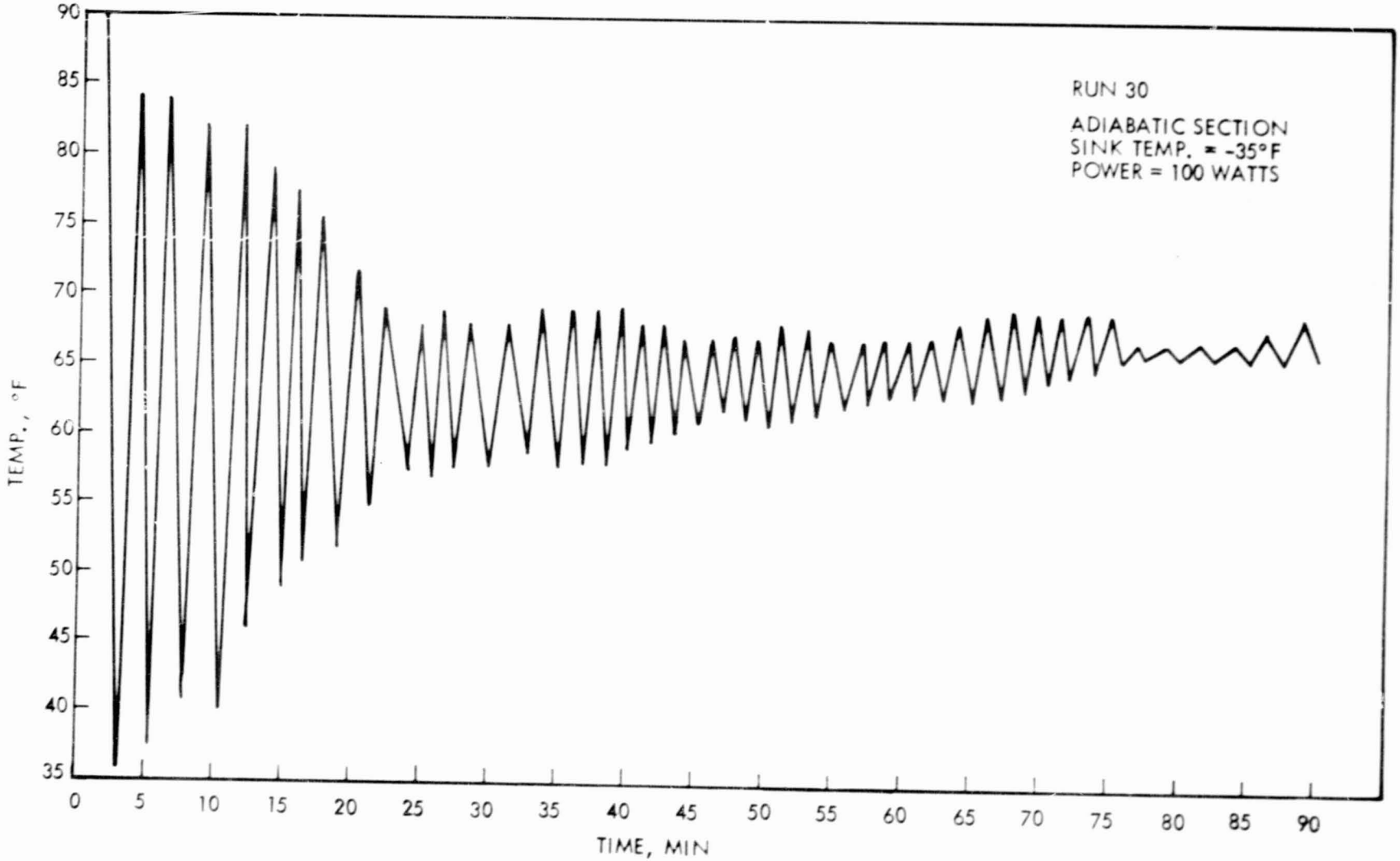

Figure 2.6. Transient Response of Input Heat Pipe for -35°F Sink

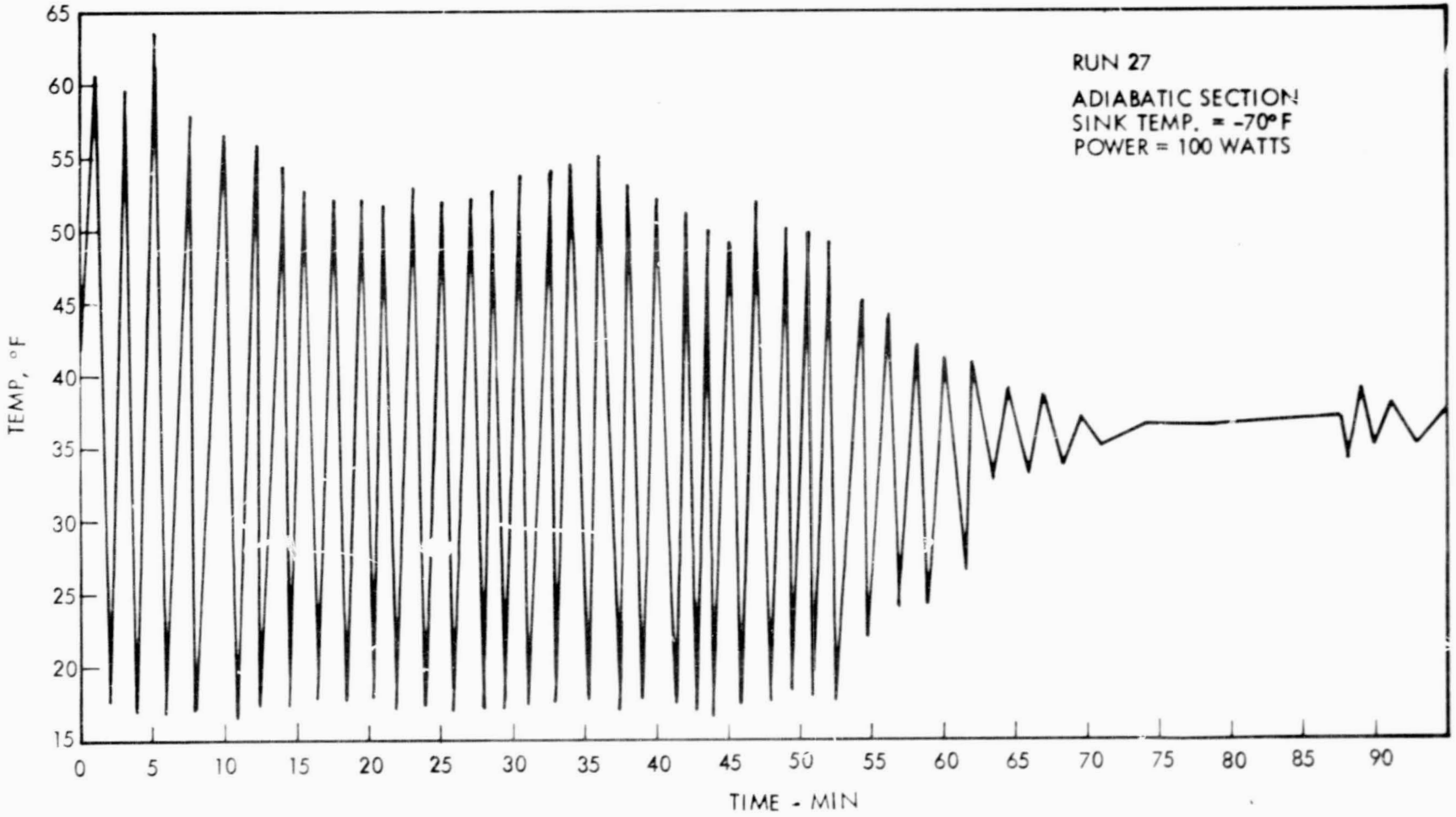

Figure 2.7. Transient Response of Input Heat Pipe for -70°F Sink

ORIGINAL PAGE IS
OF POOR QUALITY

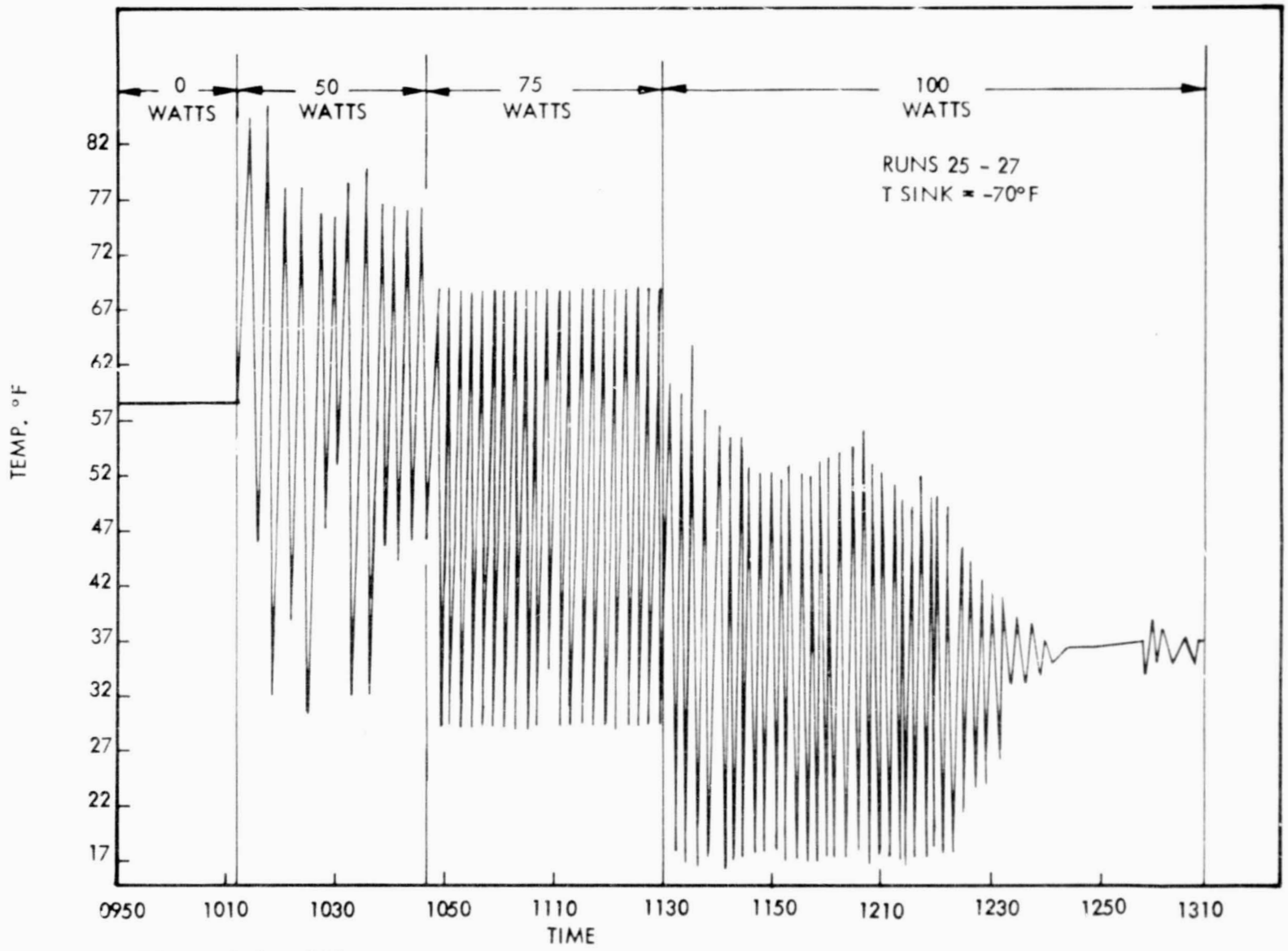

Figure 2.8. Effect of Power on Stability of Input Heat Pipe Adiabatic Temperature

2.2.3.3 The Power Input.

With a large source mass, the response of the heat pipe to a step change in power was characterized in general by a single damped temperature oscillation with a period of less than 10 minutes followed by steady operation at a temperature level that decreased with increasing power. The decrease of the operating temperature at higher power is attributed to the higher operating temperature of the sensor which results in lower pressure drops across the valve. Small source mass runs showed that the response of the heat pipe to a step change in power is generally characterized by temperature oscillations. The amplitude and frequency of these oscillations depend on the power level and other operating parameters, particularly the volume of the sensor and the sink temperature. From Table 2.2, it can be seen that the period of the oscillations decreases with increasing power, which tends to favor stability. The stabilizing effect of high power can be seen in Figure 2.8, where the input heat pipe adiabatic temperature is shown as the MVHP was operated with the larger sensor volume and the condenser close-coupled to the sink at -70°F. As shown, the large, variable-amplitude oscillations observed at 50 watts become stable at 75 watts and critically damped at 100 watts.

Analyzing the results from Runs 19 through 24, it can be seen that high power can have a dampening effect on temperature oscillations provided the sink temperature is sufficiently low.

2.2.3.4 The Sensor Volume.

One of the original objectives in the experimental investigation of the thermal response of VMHP was to determine whether or not a larger sensor volume could result in increased control sensitivity. The experimental results were only partially successful in resolving this issue. As seen in Table 2.2, the results with the larger sensor, Runs 25 through 42, show that the set point increased continuously during this phase of testing. As a result, a viable comparison between the two sensors cannot be made.

Comparing Runs 13 through 24 to Runs 25 through 42, it can be seen that under similar operating conditions, the performance of the heat pipe with the smaller sensor is significantly more stable than with the larger sensor. This fact can be construed as resulting from the higher sensitivity of the larger sensor.

High source mass Runs 34 through 42 show that the set point shifts upwards as the sink temperature is increased. It is surmised that the larger fluid volume expansion in the larger sensor, particularly during source temperature overshoots, could have caused permanent enlargement of the volume of the bellows subsequently requiring higher sensor operating temperatures to open the valve. This seems to be supported by the experimental results. If this is correct, the larger sensor exceeded the design constraints of the valve/bellows assembly of the present vapor-modulated heat pipe.

2.3 Investigation of the Use of Non-Condensible Gas

During tests of the VMHP conducted under the previous contract, reduction of the sink temperature below the freezing point of the working fluid caused the heat pipe to fail. A proposed solution to the freezing-point limitation was to add non-condensible gas into the output heat pipe.

2.3.1 Theoretical Analysis

In principle, as the active portion of the output heat pipe falls in temperature, the gas expands and blocks an increasingly longer region of the condenser. While the gas blocked region can freeze, the active portion is kept above the freezing point, and the condensing liquid is free to circulate. The flat-front theory can be used here to estimate the amount of gas required. Assuming that at maximum heat load and highest sink temperature the active vapor temperature of the output heat pipe is 70°F and a gas reservoir is at 60°F, and under minimum load and the lowest sink conditions the active vapor temperature is -100°F with the sink at -200°F, then the required reservoir-to-condenser ratio is 0.13. Because of this small ratio, the gas can be simply stored at the end of the condenser. For a condenser section 24 inches long, the required amount of gas is approximately 5×10^{-7} lb-mole.

2.3.2 Experimental Results

During the transient response test runs, it was found that some gas was present in the output heat pipe as indicated by temperature gradients in the condenser section. This gas was vented prior to the final transfer of the calculated amount of nitrogen gas into the output heat pipe.

The VMHP was instrumented with thermocouples as in previous test runs, and was tested with the high source mass and the condenser thermally close-coupled to the cold plate which was cooled with liquid nitrogen. The performance of the heat pipe under various heat loads and sections of the condenser below the freezing temperature of the working fluid is shown in Figure 2.9. At 20 watts, the adiabatic temperature of the input heat pipe is seen to oscillate about a mean temperature of 80°F with an amplitude and frequency which remain steady for more than 2.5 hours with most of the condenser frozen. As the power is increased to 50 watts, the temperature oscillations are damped followed by steady operation with most of the condenser still frozen. At 100 watts, the gas front is seen to move past TC 13. Steady temperature control can be observed for 40 minutes with more than half of the condenser below the freezing point. Thereafter, the flow of liquid nitrogen was interrupted to allow the condenser to warm up. For the next two hours, as the sink temperature increases from -157°F to 25°F, the input heat pipe adiabatic temperature is seen to remain essentially undisturbed by the large changes in sink conditions pointing to the excellent control characteristics of the VMHP.

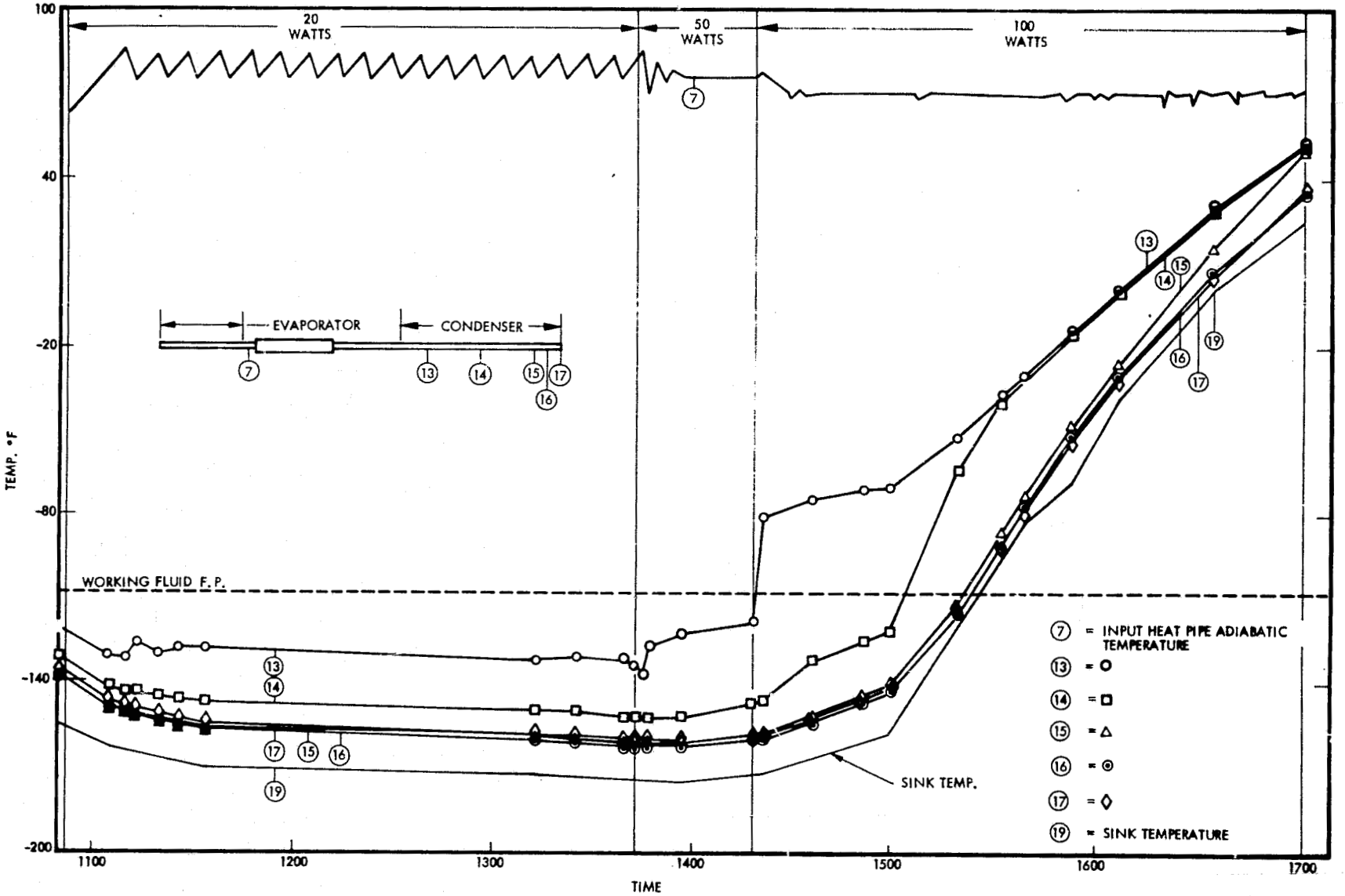

Figure 2.9. VMHP Performance at Sub-freezing Conditions

ORIGINAL PAGE IS
OF POOR QUALITY

2.4 Theoretical Investigation of Transient Response

2.4.1 Discussion

Transient test results of the vapor modulated heat pipe show cyclic adiabatic temperature profiles that can be used as a basis for formulating an analytical model of the valve performance. Figure 2.10 is copy of data obtained during the freezing point testing. Portions of the curve are labeled for ease of discussion.

The postulated phenomena causing this profile are: At point A the valve closes and the vapor space in the evaporator starts to be pressurized by the still-evaporating liquid. The rise in vapor pressure causes a rise in wetted-wall temperature, and the heat flow from the evaporator mass to the evaporator wall is reduced, while the source heat flow continues. The difference between the two heat flows causes the evaporator mass to be heated transiently. The rate of heating is reduced by the remaining evaporative cooling as the vapor is compressed and blows liquid out of the evaporator wick and vents through the wick to the condenser.

The continued evaporation and loss of liquid blown through the valve bulkhead causes the wick to desaturate. With continued desaturation, eventually a vapor-liquid pressure difference (stress) is achieved sufficient to prevent capillary pumping up the evaporator wall grooves. The groove dry-out at point B eliminates the bulk of the evaporative cooling, and the bulk of the heat flow goes into transient heating of the evaporator mass. The slope of the temperature-time curve becomes steep .

As the evaporator mass heats up, the thermosat volume heats up too, but with a time lag. Eventually the thermostat heats up sufficiently to open the valve enough for the meniscus bridging it to rupture, and vapor evaporated on the evaporation side of the valve is vented, allowing liquid to rewet the wick. The rewetting of the wick gives some cooling, perhaps from boiling in the wick, and the cooling reduces the rate of temperature rise at point C. The full length of the wick is rewet at point D.

The wick saturates sufficiently to allow the grooves to reprime, rewetting the evaporator wall at point E. Now the cooling is rapid. As the evaporator-

ORIGINAL PAGE IS
OF POOR QUALITY

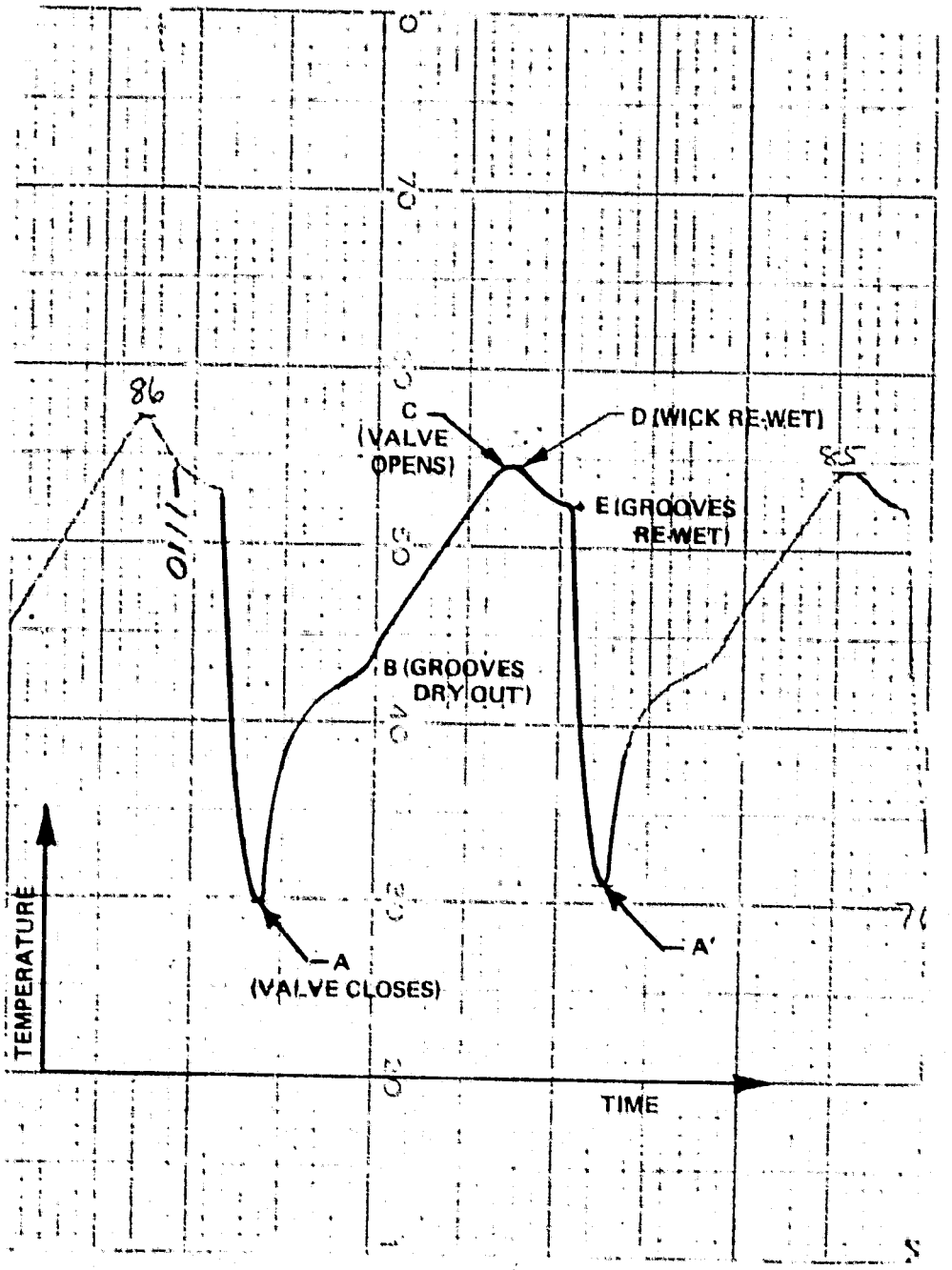

Figure 2.10. Temperature Fluctuations in a Vapor-Valve-Controlled Heat Pipe

ORIGINAL PAGE IS
OF POOR QUALITY

mass temperature falls, so does the thermostat temperature, but with a time lag. Eventually the thermostat closes the valve at point A', and the cycle repeats.

It is desired to computer-model the transient behavior in order to quantify the preceeding qualitative explanation. If the computer model agrees reasonably well with the observed behavior, then the phenomena are probably understood, and the effects of various system parameters such as evaporator mass and thermal resistance can be determined.

2.4.2 Mathematical Model Elements

Equipment and Heat Source. For simplicity the equipment and heat source will be modeled as a single lumped capacity C_1 heated at rate $\dot{Q}$ and cooled by thermal coupling to the vapor space at temperature T_v. The thermal coupling to T_v is by a main path to the evaporator wall and an auxiliary path via the evaporator wick. A minor shunt conductance representing conduction to the condenser may be assumed as well, of course, the thermostat acts as a minor heat sink during transient warmup. Figure 2.11 illustrates the model and Eq. (1) gives the governing equation:

$$C_1 \frac{dT_1}{dt} = \dot{Q} - \dot{Q}_{1-e} - \dot{Q}_{1-2} \tag{1}$$

where

$$\dot{Q}_{1-e} = \frac{T_1 - T_e}{R_i + \dfrac{1}{\dfrac{1}{R_s} + \dfrac{1}{R_v + \dfrac{1}{\dfrac{1}{R_g} + \dfrac{1}{R_w}}}} + R_o + R_e} \tag{2}$$

ORIGINAL PAGE IS
OF POOR QUALITY

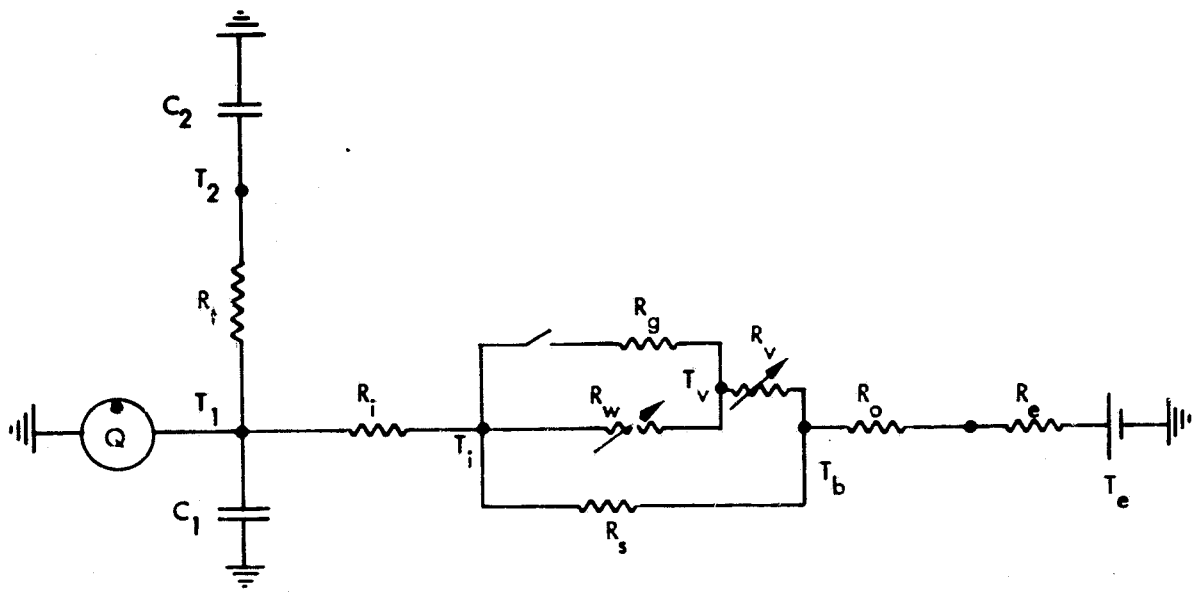

C_1	Equipment-mass thermal capacity
C_2	Thermostat thermal capacity
R_i	Input heat pipe resistance
R_t	Thermostat coupling resistance
R_g	Grooved wall resistance (negligible)
R_w	Wick resistance
R_s	Shunt resistance
R_v	Vapor valve resistance (nonlinear)
R_o	Output heat pipe resistance
R_e	External condenser resistance

Figure 2.11. Thermal Model

and

$$\dot{Q}_{1-2} = \frac{1}{R_t} (T_1 - T_2) \tag{3}$$

Thermostat. The thermostat is also modeled as a single lumped capacity.

$$C_2 \frac{dT_2}{dt} = \frac{1}{R_t} (T_1 - T_2) \tag{4}$$

Grooves. The grooves are modeled with a switch U_g that is either on or off and resistance R_g. Of course, the grooves could be modeled as a number of such subelements, but one is thought sufficient for a first-stage model. The switch U_g is equal to either 0 or 1 and is imagined to be a function of vapor-to-liquid pressure difference $P_v - P_l$ which in turn is a function of the liquid remaining in the wick m_l.

$$U_g = \begin{cases} 0, & m_l \leq m_{crit,\ grv} \ (=m_{small})^* \\ 1, & m_l > m_{crit,\ grv} \ (=m_{small}) \end{cases} \tag{5}$$

Valve. For simplicity the valve is modeled as either open or closed. When the valve is opened $R_v = 0$. (This crude feature of the model can be refined later.) When the valve is closed the vapor must blow through the large pores in the wick, and the vapor flow is modeled as subsonic Darcy flow through a porous plug.

*In the two-pore model to follow.

$$R_v = \frac{T_v - T_b}{\dot{Q}} = \frac{T_v - T_b}{\dot{m}_v h_{fg}} = \frac{T_v - T_b}{h_{fg}\rho_v A \frac{2D^2}{\mu_v K L_v \tau}\left[P_{vap}(T_v) - P_{vap}(T_b)\right]}$$

$$R_v = \frac{T_v - T_b}{H_{fg}\rho_v A \frac{2D^2}{\mu_v K L_v \tau}\left[P_{vap}(T_v) - P_{vap}(T_b)\right]}, \quad T_2 < T_{set} \tag{6a}$$

$$R_v = 0, \quad T_2 \geq T_{set} \tag{6b}$$

For convenience the Clausius - Clapeyron equation may be used for $P_{vap}(T)$.

$$P_{vap}(T) = P_o \exp\left[\frac{h_{fg}}{RT_o}\left(1 - \frac{T_o}{T}\right)\right] \tag{7}$$

It is necessary to find T_v and T_b from Figure 2. For example

$$T_v = T_i - \left[\dot{Q}_{1-e} - (T_i - T_b)/R_s\right]\left[1/(R_w^{-1} + R_g^{-1})\right] \tag{8}$$

Wick. The mass of liquid in the wick controls groove wetting through Eq. (5), and R_w through a relation yet to be specified. The liquid remaining in the wick is controlled by liquid flow out (or in) and the rate of vaporization. A two-pore model may be used for simplicity in representing the wick. The wick is imagined to have a cross section of A of big pores of size D and one of a of small pores of size d. (1) The wick can be fully saturated in which case both areas are filled over the entire length L. (2) The wick can be big-pore desaturated in which case A is only partly filled uniformly over the entire length L. (3) The wick can be small-pore desaturated in which case area A is dry and area a is fully filled over only part of length L.

ORIGINAL PAGE IS
OF POOR QUALITY

The equation for m_l is simply

$$\frac{dm_l}{dt} = - \dot{m}_{evap} + \dot{m}_{in} \tag{9}$$

The quantity $\dot{m}_{evap}$ is given by the circuit in Figure 2.11.

$$\dot{m}_{evap} = \dot{Q}_{evap}/h_{fg} \tag{10a}$$

$$\dot{Q}_{evap} = \frac{T_i - T_b}{R_v + \frac{1}{\frac{1}{R_g} + \frac{1}{R_w}}} \tag{10b}$$

$$T_i = T_l - \dot{Q}_{l-e} R_i \tag{10c}$$

$$T_b = T_e + \dot{Q}_{l-e} (R_e + R_o) \tag{10d}$$

The quantity $\dot{m}_{in}$ is more complex. Three cases corresponding to the three states of the wick must be considered. In general, however,

$$\dot{m}_{in} = \left[\frac{4 D^2 \rho_l}{K\tau\mu_l L} f_{wet} A + \frac{4 d^2 \rho_l}{K\tau\mu_l L_{wet}} a\right] \left[\frac{4\sigma}{D_{men}} - \Delta P_v\right] \tag{11}$$

$$\Delta P_v = P_{vap}(T_v) - P_{vap}(T_b)$$

For the wick to be full, the valve must be open (but not necessarily vice versa). Under these conditions the following valves exist:

$$f_{wet} = 1,\ L_{wet} = L,\ T_v = T_b \text{ so } \Delta P_v = 0$$

$$D_{men} \geq D\ ,\ m_l = m_{full},\ U_g = U_w = 1 \tag{12}$$

The meniscus diameter-of-curvature adjusts so that $dm_l/dt = 0$. Recall that this situation was imagined to occur between E and A' in Figure 2.10. After the valve closes the large pores begin to desaturate, because T_l heats up transiently due to the reduced value of R_v, and eventually $T_v - T_b$ increases to the extent that

$$\Delta PV > \frac{4\sigma}{D}$$

Even before this condition, Eq. (9) will have gone to negative value of dm_l/dt. With $m_{small} < m_l < m_{full}$, we have

$$f_{wet} = \frac{m_l - m_{small}}{m_{full} - m_{small}} \; ; \; L_{wet} = L, \; D_{men} = D, \; U_g = U_w = 1 \qquad (13)$$

With continued operation at negative dm_l/dt, the value of m_l falls below m_{small},

$$m_l < m_{small} \quad f_{wet} = 0 \quad D_{men} = d$$

$$U_g = 0 \quad U_w = L_{wet}/L$$

$$L_{wet}/L = m_l/m_{small} \qquad (14)$$

When the valve reopens ΔP_v falls to zero, and dm_l/dt becomes positive. Until m_l reaches m_{small}, the conditions of Eq. (14) remain in force. When m_l exceeds m_{small}, Eq. (13) comes into play. Finally, when m_l reaches m_{full}, the conditions of Eq. (12) pertain.

The value of R_w needed is taken to be simply

$$\frac{1}{Rw} = \frac{1}{R_{wo}} U_w \qquad (15)$$

where R_{wo} is for boiling in the full wick.

2.4.3 Computer Program Elements and Organization

Main Program. The main program is visualized to read in the required data, initialize the variables, and then repeatedly call a subroutine to execute a Runge-Kutta forward marching in time. The time-temperature history is written as output.

Runge. The main subroutine is thus visualized to be subroutine Runge, which calls Subroutine Delta four times and averages the results. The main variables are equipment temperature T_1, thermostat temperature T_2, and mass of liquid in the wick m_1.

Delta. Subroutine Delta computes the derivatives dT_1/dt, dT_2/dt, and dm_1/dt using Eq. (1), Eq. (4), and Eq. (9) respectively. Functions or subroutines must be used to solve (given T_1, T_2 and M_1) for R_v, R_g, R_w, and T_v and T_b. Subroutine Test may be used to find R_g and T_w versus m_1, and Subroutine Relax may be used to find T_v, T_b, and R_v.

Test. Subroutine Test is visualized to find R_g and R_w versus m_1 by employing Eqs. (12), (13), or (14) depending upon whether $m_1 = m_{full}$, $m_{small} \leq m_1 < m_{full}$, or $m_1 < m_{small}$.

Relax. Subroutine Relax must solve the nonlinear problem of finding T_b given by Eq. (10d) and T_v given by Eq. (8), with Eqs. (10bc), and R_v given by Eq. (6a) or (6b). It is thought that a relaxation procedure can be used or quasilinearization.

Pvap. Function Pvap computes the vapor pressure from Eq. (7) or a more accurate fit to vapor pressure data.

Two-Pore-Model Parameter Estimations.

Use of the two-pore model requires specifying six parameters: a, A, d, D, $(K\tau)_1$, and $(K\tau)_2$ appearing Eqs. (6a) and (11). There are only two main constraints (1) that the areas sum to the total void area and (2) that the permeability agree with the measured value.

$$a + A = \varepsilon_v A_{wick} \tag{16}$$

$$KA_{wick} = \frac{2D^2}{(K\tau)_1} A + \frac{2d^2}{(K\tau)_2} a \tag{17}$$

ORIGINAL PAGE IS
OF POOR QUALITY

Four arbitrary conditions must be imposed to complete the description. These are

$$a = A \tag{18}$$

$$(K\tau)_1 = (K\tau)_2 \tag{19}$$

$$D = 2d \tag{20}$$

$$d = 2\delta \tag{21}$$

where δ is the fiber diameter of a fibrous wick. The last condition is chosen in view of the fact that Eninger's theory for fibrous wicks has

$$\frac{\Delta P\delta}{\sigma} \doteq \frac{3}{2}$$

where we desire

$$\frac{\Delta Pd}{\sigma} \doteq 3$$

For consistency with the proposed model of groove dry-out occurring after partial wick desaturation it is necessary that the equivalent groove pumping diameter D_{cr} fall between D and d.

where

$$\frac{4\sigma}{D_{cr}} = \frac{\sigma}{R}\ ,\ R = \frac{W_{1/2}}{\cos\Theta_{1/2}}$$

The quantity $W_{1/2}$ is the half groove width, and $\Theta_{1/2}$ is the half groove angle. For a 5 mil fiber diameter δ, a 7 mil groove width and a 19 degree groove half angle we find compatibility, for

$$D = 20 \text{ mils};\ d = 10 \text{ mils};\ D_{cr} = 14.8 \text{ mils}.$$

2.4.4 Results and Conclusions

A computer program was developed which incorporates the elements and the organization outlined in the previous section. A listing of the Fortran IV version of this program is given in Appendix B. Attempts to obtain physically realizable solutions failed due to numerical instabilities; as a result, the soundness of the postulated model could not be verified. It appears that the relaxation procedure used in the program is too simple in view of the strong nonlinearities in the mathematical model. A possible solution to the numerical problems is the linearization of the model by techniques such as quasilinearization. However, this effort was beyond the scope of the present contract. Since the two-pore model proposed is believed to be conceptually complete, continued program development is recommended.

3. DEVELOPMENT OF VAPOR INDUCED DRYOUT DIODE HEAT PIPE

3.1 INTRODUCTION

Heat pipes are self-contained devices that transport heat at a high rate between a source and a slightly cooler sink. In some applications, it is desirable to have the heat pipe transfer heat in only one direction; that is, when the source is warmer than the sink, the heat pipe would act in its normal high conductance mode, but when the sink temperature rises above the source, the heat pipe would turn off and act as an insulator. Thus, the heat pipe acts as a diode. An example is the cooling to cryogenic temperature of an infra-red detector on a satellite. A diode heat pipe couples the detector to a space radiator that radiates to deep space. When the sun shines on the radiator, it becomes much warmer than the detector, and the heat pipe turns off, thus preventing the detector from warming up.

Currently, there are three mechanisms that are used to achieve diode behavior in heat pipes:

1. Gas Blockage - In the forward mode, a reservoir at the end of the condenser is used to store noncondensible gas. In the reverse mode, the gas blocks the region of the heat pipe at the source.

   Disadvantage - A very large gas reservoir is required, especially for cryogenic applications.

2. Liquid Trap - In the reverse mode, liquid is condensed in an unwicked volume near the source and the wick dries out.

   Disadvantage - A large excess-liquid reservoir is required and considerable heat is transferred in the reverse mode before the wick dries out.

3. Excess Liquid Blockage - In the forward mode, excess liquid is stored in a reservoir at the end of the condenser. In the reverse mode, the excess liquid fills the vapor space in the region of the source and prevents heat transfer.

   Disadvantage - A reservoir is required and heat is transferred in the reverse mode to evaporate and condense the excess liquid. Also, it is not well suited for a slab-wick heat pipe.

A fourth mechanism reported here for achieving diode behavior has none of the disadvantages of the other three mechanisms. This mechanism was developed under the present contract: a vapor-induced dryout diode using vapor modulation by means of a metal-foil reed valve.

3.2 BASIC OPERATING PRINCIPLE

The mechanism that was previously used successfully for passive feedback temperature control, which is based on the vapor-induced dryout principle, is depicted in Figure 3.1. Although this design differs somewhat from the one selected for fabrication, it has essentially the same basic features and is presented here to illustrate the diode mechanism and as a possible alternative design.

A conventional non-arterial slab-wick heat pipe has a metal-foil reed valve in its transport section. In the forward mode, the reed valve is designed to open at a pressure differential which is small compared to the capillary pressure limit of the wick. Returning liquid from the evaporator bypasses the valve bulkhead through an annular transfer wick. In the reverse mode, the valve closes. When the resulting pressure that builds up reaches the capillary pressure limit of the wick, which occurs rapidly, liquid flows from the high pressure side of the valve, through the annular wick, to the low pressure side. The region that was the condenser in the forward mode dries out and the region that was the evaporator floods with liquid.

3.3 DESIGN OF DIODE HEAT PIPE

The design is shown in SK78007 in Appendix A. A 0.50-inch O.D. graded-porosity slab-wick heat pipe has in its transport section a 1-inch O.D., 1.5-inch long cylinder which supports the valve bulkhead. The density radiation of the slab-wick with respect to length is shown in Figure A-1 in Appendix A.

In addition to its high transport capacity, the graded porosity wick has certain features that are ideally suited for the diode mechanism. The pressure available to open the valve is the high capillary pressure generated by the relatively low porosity of the evaporator region, while

ORIGINAL PAGE IS
OF POOR QUALITY

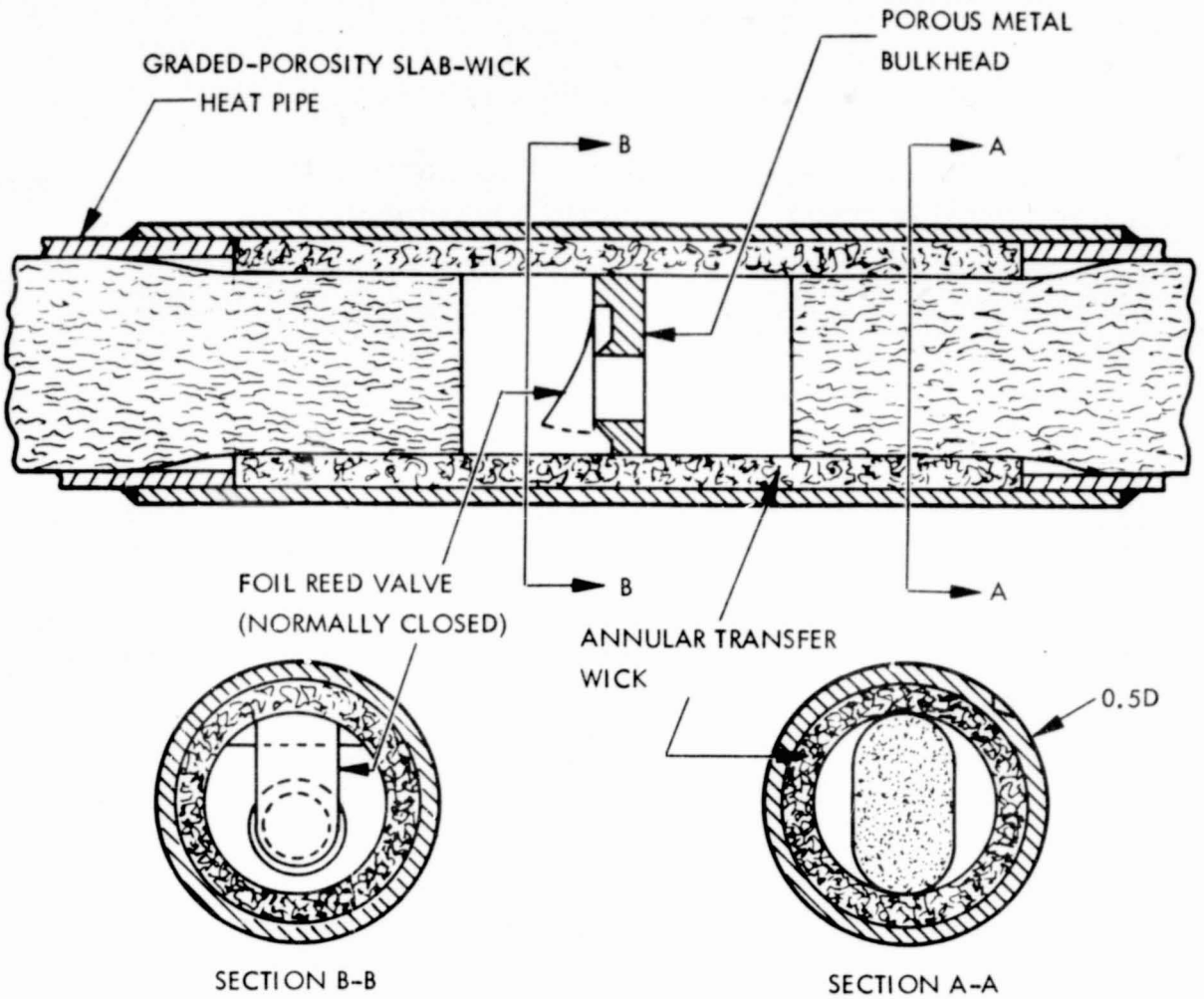

Figure 3.1. Vapor-Induced-Dryout Diode

the pressure required to induce dryout is the low capillary pressure of the relatively high porosity of the condenser region.

All components were made out 304 stainless steel. The criterion for selecting a single material to build the heat pipe diode was the ready availability of the materials and manufacturing cost. The use of aluminum tubes connected to the valve section by means of transition tubing would have been desirable from weight consideration, however, the higher manufacturing cost could not be justified at this stage when the main objective was to test the practicality of the diode mechanism.

3.3.1 The Valve Bulkhead Design

The valve bulkhead assembly before it was assembled is shown in Figure 3.2. The bulkhead has a central solid core with five orifices, a wick feed-thru orifice and four smaller orifices for the vapor flow tubes which are pressure fitted into holes in the bulkhead and pinned in place. The ends of two vapor flow tubes provide the seat for each of the two reed valves. In order to fit the valve assembly into a 1-inch O.D. cylinder and still be able to use relatively long foil flaps, the ends of the vapor flow tubes were cut at an angle placing the seat of each valve on a plane approximately 30^{o} with respect to the axis of the heat pipe. On this plane, the vapor flow crossectional area at the valve seat is about twice that at the inflow, thus only small deflections of the foil reeds are required to fully open the valve. The vapor flow tubes have a thin wall which is necessary in order for the valve seat to have a small contact area, otherwise surface tension forces due to liquid between the seat and the foil would generate an excessive force tending to keep the valve shut.

3.3.2 The Wick Feed-Thru

The wick feed-thru is shown in SK78007 and also in a photograph in Figure 3.3. Its configuration is similar to that used in the vapor-modulated heat pipe. The wick on either side of the bulkhead is separated at the bulkhead by two layers of 250-mesh screen, which form the capillary barrier. The screen is held in the center of the wide feed-thru orifice

ORIGINAL PAGE IS
OF POOR QUALITY

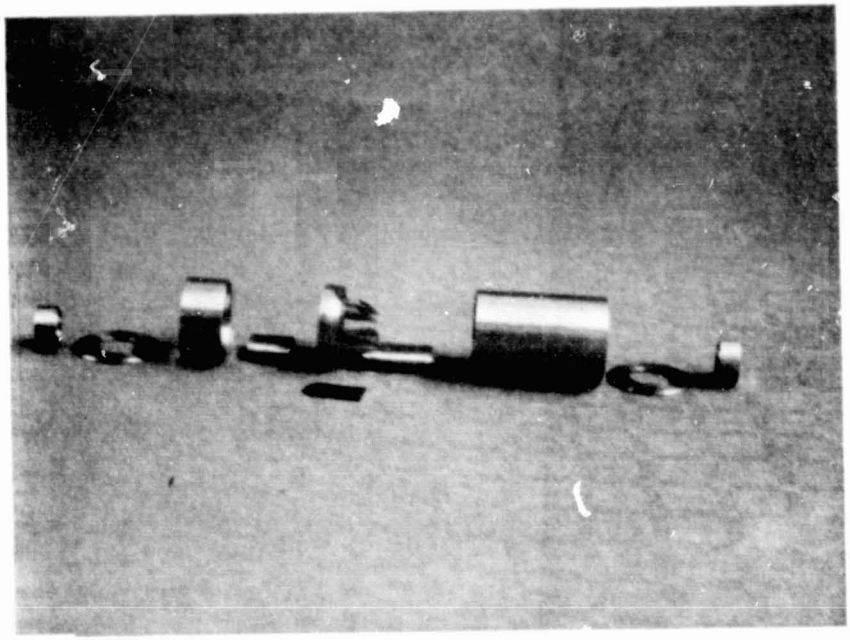

Figure 3.2 Reed Valve Bulkhead Components

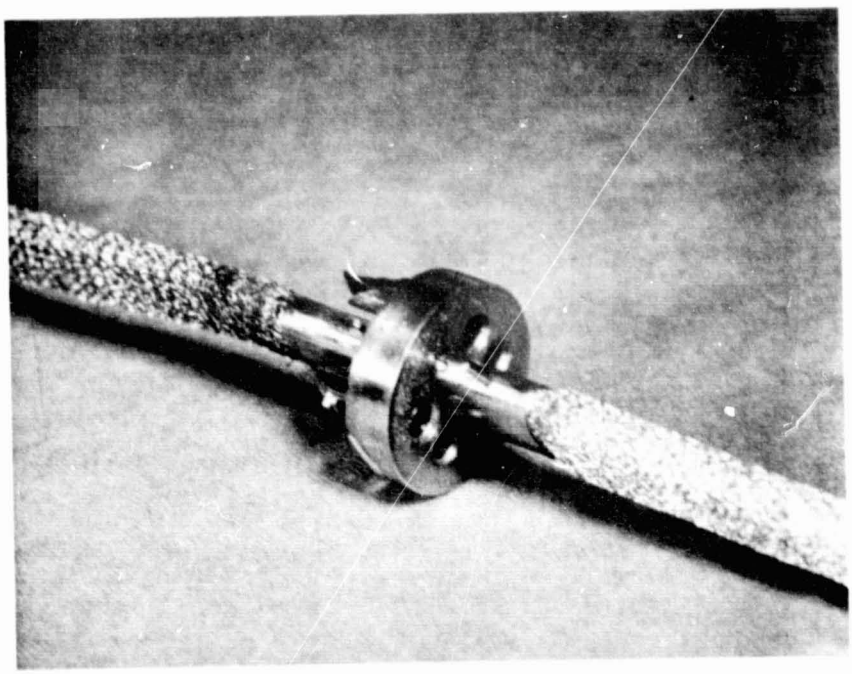

Figure 3.3 Wick Feed-Thru Assembly

by two sleeves that were inserted halfway into the orifice from both sides of the bulkhead. The sleeves were pressed together to clamp the screen in place and then were tack welded to the bulkhead. The ends of the wicks were inserted into sleeves, trimmed flush, inserted into the bulkhead sleeves, pressed against the capillary barrier, and pinned in place.

3.3.3 Reed Valve Assembly Tests

The valve assembly was initially tested in a glass tube which allowed visual observation of its behavior. A Teflon bushing between the glass tube wall and the bulkhead provided an air-tight seal. The glass tube was instrumented to allow pressure and gas flow measurements.

Reed valves manufactured from 0.0005-inch and 0.00025-inch 304 stainless steel foils were tested, and the latter chosen due to their greater sensitivity to pressure differentials.

The effective pore size of the capillary barrier in the test assembly was determined by a bubble-point test. The wick was saturated with acetone and the reed side of the test chamber was pressurized simulating diode behavior. The pressure continued to rise until the capillary barrier failed and bubbles were observed emerging from the wick. The pressure at failure corresponds to an effective capillary pore size of 0.0035-inches. This pore size is sufficiently small to ensure that the abnormal evaporator will dryout when the valve closes in the diode mode.

Preliminary tests were performed in the forward mode in which the wick was saturated with acetone, the valve seats were wet, and helium gas was used to simulate the vapor flow. It was observed that only one of the valves would open. This behavior was attributed to the permanent set of one of the foil reeds opposing outward deflection of the foil and/or large capillary forces keeping the foil adhered to the valve seat. The foil flaps were subsequently placed between two metal blocks and annealed. This operation resulted in flat foil material.

The valve seat contact area was reduced by chemically etching the front section of the vapor flow tubes.

The valve assembly was then reassembled and subjected to further tests. Under conditions similar to those described above, it was observed that the pressure continued to rise until one of the valves opened. The pressure at which the valve opened corresponds to an effective capillary pore size of 0.026-inch. This pore size is sufficiently large to ensure that the liquid in the normal evaporator will not flow into the condenser side before the valve opens.

For a wide range of gas flow rates, the foil was found to deflect smoothly without flapping. By diverting the gas flow into the other side of the glass chamber, the valve was tested in the diode mode. The pressure would rise until the capillary limit of the barrier was reached. Simulation of heat pipe operation in the forward and diode modes in this way was repeated at least a dozen times with reproducible results.

3.3.4 Heat Pipe Diode Test Results

The heat pipe was assembled following the procedure outlined in SK78007, page 4 of 4, a photograph is given in Figure 3.4.

After a 16-hr refluxing operation at 80^{o}C, the heat pipe was vacuum baked and charged with 32.6 grams of ammonia. Subsequently the heat pipe was instrumented and tested in the forward mode. At a 0.2-inch tilt, it held 135 watts and burned out at 150 watts. This was well below the predicted capacity of over 225 watts. In addition a temperature drop was observed across the valve, which increased with increasing heat input. These two facts were evidence of an impaired function of either the wick or the valve or both.

Since structural damage to the valve was suspected, prior to conducting a detailed tilt capacity test in the forward mode, the heat pipe was tested in the reverse mode. Repeated attempts to close the valve by applying increasing power failed inasmuch as the evaporator showed no signs of dryout even at 100 watts. In fact the heat pipe operated much as in the forward mode.

The results clearly indicated the valve was damaged.

ORIGINAL PAGE IS
OF POOR QUALITY

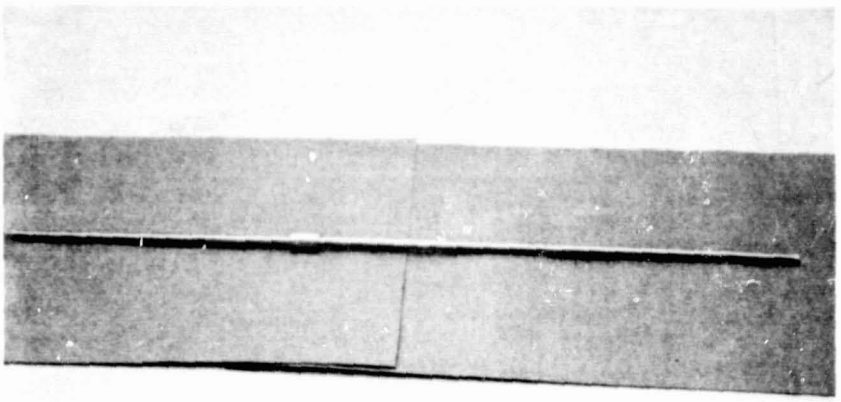

Figure 3.4 Diode Heat Pipe After Assembly

The heat pipe was subsequently dismantled. A photograph of the valve assembly is shown in Figure 3.5 where it can be readily seen that the reed valves had been severely damaged.

The foils were wrinkled and showed evidence of having been forced into the tube sections. This damage would not allow the foil to seat and therefore prevented the foils from stopping vapor flow in the reverse direction.

One additional item of damage sustained during manufacture was a hole in the wick about one inch from the bulkhead on the condenser side of the heat pipe. This hole was approximately 1/8" diameter extending approximately 2/3 of the way through the wick. The hole was darkened and was obviously the result of a burn. Apparently a molten drop of metal fell into the wick at some point during welding-most likely during one

ORIGINAL PAGE IS
OF POOR QUALITY

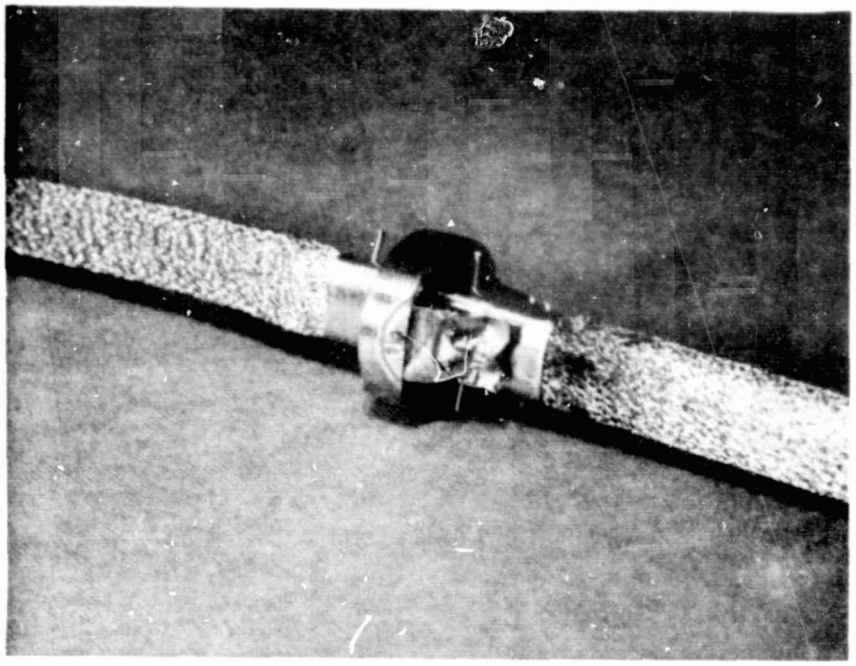

Figure 3.5 View of Damaged Reed Valve

of the repair welds made to close the leak in the valve section. The burn spot corresponded to the location of the leak. This wick damage is the likely cause of the relatively low capacity of the heat pipe (135 watts actual vs 225 watts predicted).

3.4 CONCLUSIONS

The heat pipe diode components were tested under simulated normal operating conditions and found to be a sound working mechamism. The assembled heat pipe diode failed due structural damage incurred under conditions not yet fully understood.

It is quite likely that the damage occurred during some point in the processing stages. During the routine leak check operation, a leak had been detected in the area where the 1/2 inch O.D. tube is welded to the end cap of the valve section. In the process of finding the location of the pinhole, there was an accidental pulse pressurization of the heat pipe.

The sudden pressure differential sustained across the valve would have caused the valve to bend open, but a resultant shock wave could have impelled the foil back against the valve seat with a force sufficient to cause the observed damage.

Another possibility is that damage occurred during the refluxing step during which the pressure fluctuations associated with the unstable nature of pool boiling could have caused the foil to implode against the valve seat.

The successful testing at the component level of the metal-foil reed valve and the high capacity of the metal-fiber wick system still make this diode mechanism attractive. Re-work of the parts and careful processing of the diode seem warranted to more fully evaluate its performance.

APPENDIX A

CONTENT

SK78007 - GRADED POROSITY HEAT PIPE DIODE ASSEMBLY
SK741001 - TUBE, GROOVED
SK741024 - END CAP AND FILL TUBE
SK75061 - VAPOR-MODULATED HEAT PIPE INSTRUMENTATION
FIGURE A-1 - HEAT PIPE DIODE GRADED-POROSITY WICK

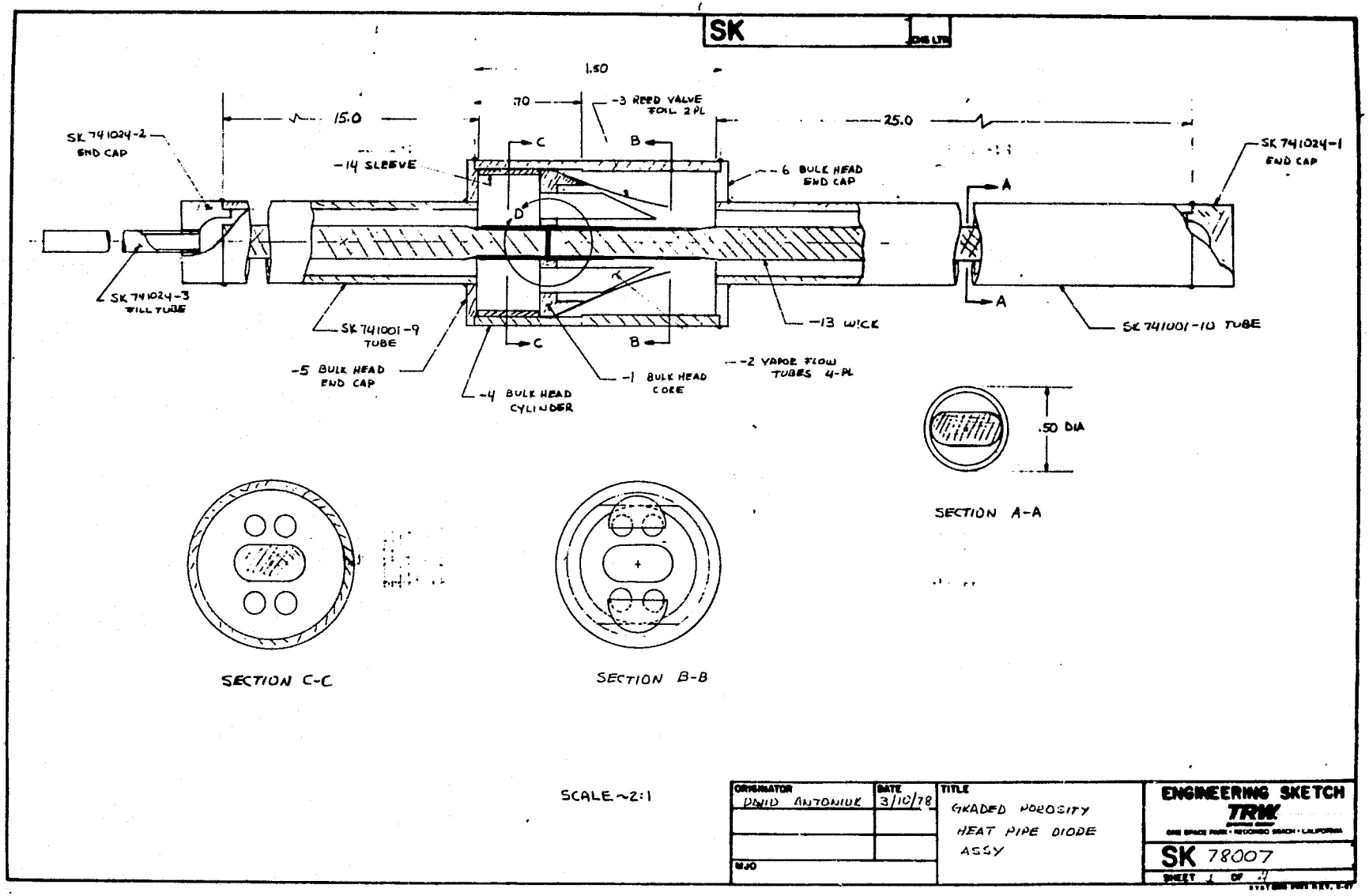

ORIGINAL PAGE IS
OF POOR QUALITY

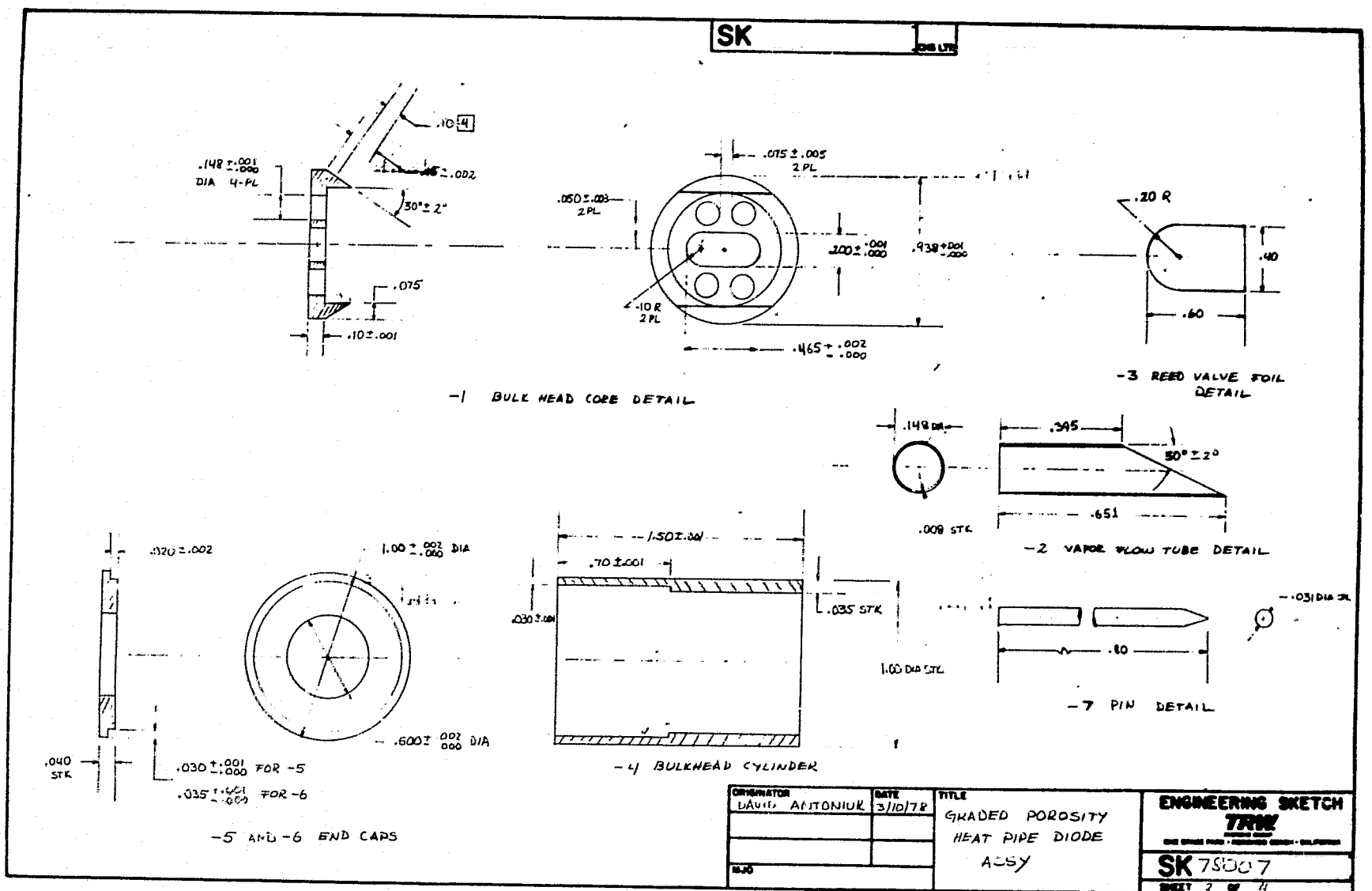

ORIGINAL PAGE IS
OF POOR QUALITY

SK

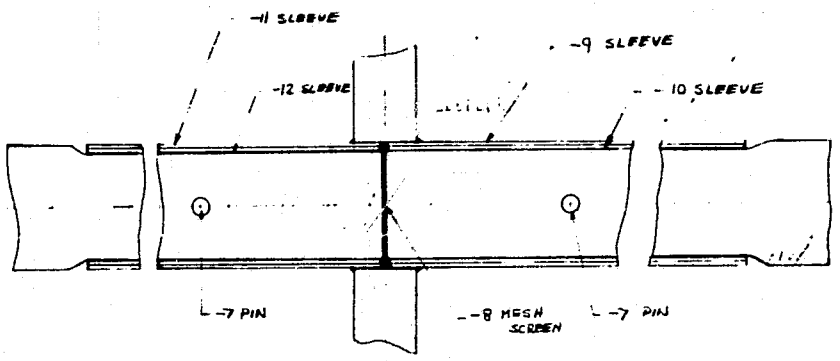

DETAIL D

WICK FEED-THRU ASSY

SCALE ~ 6/1

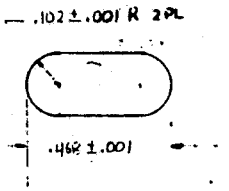

-8 MESH SCREEN DETAIL

SCALE ~ 3/1

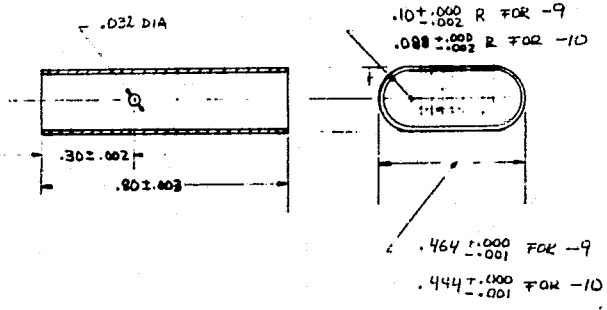

-9 BULKHEAD SLEEVE AND -10 WICK SLEEVE DETAILS

SCALE ~ 3/1

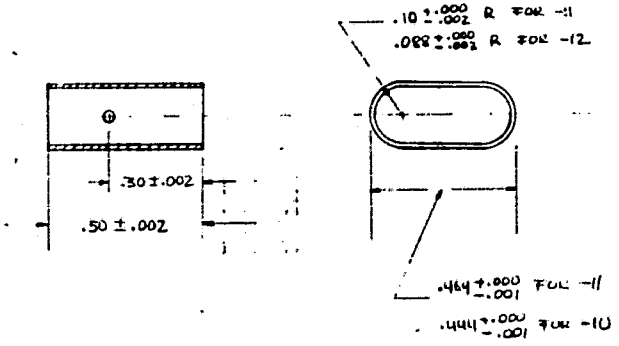

-11 BULKHEAD SLEEVE AND -12 WICK SLEEVE DETAILS

SCALE ~ 3/1

ORIGINATOR	DATE	TITLE	ENGINEERING SKETCH TRW
V. ANTONUK		GRADED POROSITY HEAT PIPE DIODE ASSY	SK 78007
			SHEET 3 OF 4
MJB			

ORIGINAL PAGE IS
OF POOR QUALITY

SK

NOTES:

1. CLEAN ALL PARTS PER PR2-28-1
2. TACK WELD OR PIN -2 TUBES TO -1 CORE
3. WELD -9 AND -11 SLEEVES TO -1 CORE AFTER RESISTANCE FITTING TWO -8 MESH SCREENS
4. TACK WELD -3 FOIL VALVE TO -1 CORE 2PL
5. SPLICE -13 WICK, INSERT INTO -10 AND -12 SLEEVES, TRIM WICK FLUSH, INSERT INTO -9 AND -11 SLEEVES RESPECTIVELY AND PIN WITH -7
6. WELD -5 CAP TO SK741001-9 TUBE AND -6 CAP TO SK741001-10 PER PR-1
7. INSERT -1 BULKHEAD AND -14 SLEEVE INTO -4 CYLINDER
8. SLIDE, SK741001-9 AND SK741001-10 TUBES OVER -13 WICK AND WELD -5 AND -6 END CAPS TO -4 CYLINDER PER PR-1
9. WELD SK741024-1 END CAP TO SK741001-10 TUBE, SK741024-2 END CAP TO SK741001-9 TUBE, AND SK741024-3 FILL TUBE TO SK741024-2 END CAP PER PR-1

PART NO.	QTY REQ'D	DESCRIPTION	MATERIAL
SK741024-3	1	FILL TUBE	304 SS 1/8 O.D. X .020 WALL
SK741024-2	1	TUBE END CAP	304 SS 1/2 DIA BAR
SK741024-1	1	TUBE END CAP	304 SS 1/2 DIA BAR
SK741001-9	1	GROOVED TUBE	304 SS 1/2 O.D. X .028 WALL TUBE
SK741001-10	1	GROOVED TUBE	304 SS 1/2 O.D X .028 WALL TUBE
-14	1	BULKHEAD SUPPORT SLEEVE	304 SS 1.0 DIA BAR
-13	1	GRADED POROSITY WICK	304 SS .005 DIA FIBER
-12	1	WICK SLEEVE	304 SS .352 O.D X .020 WALL
-11	1	BULKHEAD SLEEVE	304 SS 3/8 O.D. X .012 WALL
-10	1	WICK SLEEVE	304 SS .352 O.D X .020 WALL
-9	1	BULKHEAD SLEEVE	304 SS 3/8 O.D. X .012 WALL
-8	2	MESH SCREEN	304 SS 250 MESH SCREEN
-7	2	PIN	304 SS 1/32 DIA ROD
-6	1	BULKHEAD END CAP	304 SS .040 THK SHEET STOCK
-5	1	BULKHEAD END CAP	304 SS .040 THK SHEET STOCK
-4	1	BULKHEAD CYLINDER	304 SS 1.0 O.D. X .035 WALL TUBE
-3	2	FOIL REED VALVE	304 SS .00027 THK FOIL
-2	4	VAPOR FLOW TUBE	304 SS .148 O.D. X .005 WALL TUBE
-1	1	BULKHEAD CORE	304SS 1.. DIA BAR STOCK

PARTS LIST

ORIGINATOR	DATE	TITLE
D. ANTONIDE		GRADED POROSITY HEAT PIPE DIODE ASSY
MJO		

ENGINEERING SKETCH
TRW
SK 78007
SHEET 4 OF 4

ORIGINAL PAGE IS OF POOR QUALITY

NOTES:

1. SELECT TUBES FOR NOMINAL I.D. $^{+.005}_{-.000}$ DIMENSION.
2. INTERNAL GROOVE ENTIRE LENGTH PER SP-13B-02.

SK 741001 DWG LTR

DASH NO.	L	T (STR.)
-1	35.75	0.035
-2	23.55	0.035
-3	35.88	0.035
-4	70.86	0.035
-5	38.5	0.028
-6	60.00	0.035
-7	15.50	0.035
-8	30.8	0.035
-9	15.00	0.028
-10	25.00	0.028

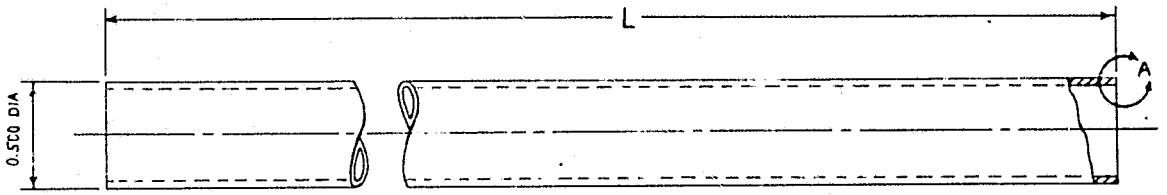

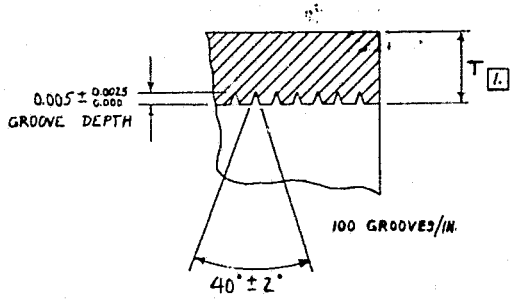

DETAIL A (20~1)

LETTER	MATERIAL	SPEC
C	PH15-7 Mo S.S.	
B	304 CRES	AMS5560
A	6061-T6 AL	WW-T-700

ORIGINATOR	DATE	TITLE
G FLEISCHMAN	10-1-74	TUBE, GROOVED - HEAT PIPE
MJO		

ENGINEERING SKETCH
TRW
SK 741001
SHEET OF

ORIGINAL PAGE IS
OF POOR QUALITY

SK	REVISIONS			
	LTR	DESCRIPTION	DATE	APPROVED

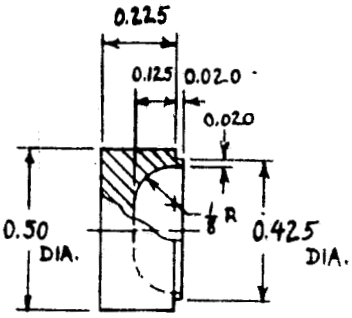

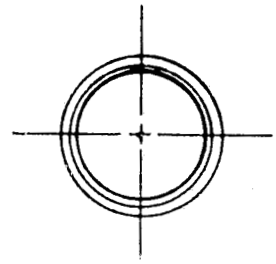

-1

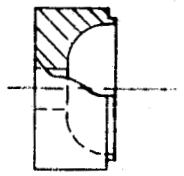

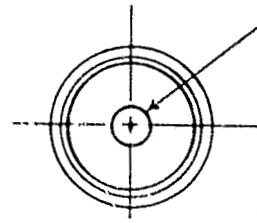

-2

-2 SAME AS -1, EXCEPT AS NOTED.

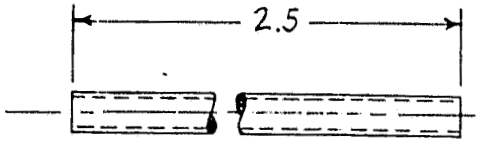

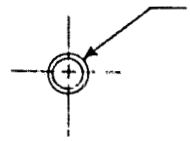

-3

PART NO.	DESCRIPTION	MATERIAL
SK741024-3	FILL TUBE	304 TUBE, 0.125 O.D. X 0.020 WALL
SK741024-2	END CAP	304 CRES ROD, 0.500 DIA.
SK741024-1	END CAP	304 CRES ROD, 0.500 DIA.

ENGINEERING SKETCH

TRW SYSTEMS GROUP
ONE SPACE PARK • REDONDO BEACH, CALIFORNIA

ORIGINATOR	DATE
G. FLEISCHMAN	10/24/74
MJO	

END CAPS AND FILL TUBE

SIZE	CODE IDENT NO.	
A	11982	SK 741024

SCALE 2~1 | SHEET 1 OF

SYSTEMS 523 REV. 12-71

SK	REVISIONS		26263-6021-RU-00	
	LTR	DESCRIPTION	DATE	APPROVED

Note: • Use 0.006" Teflon tape between input heat pipe and heater block.
• Use RTV or thermal grease between output heat pipe and heat sink

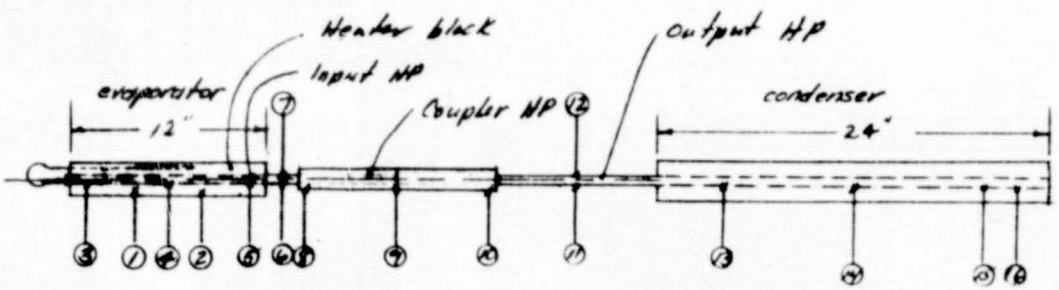

TC	Description	Location
1	Heater block	4 in. from L.H.S. of Heater block
2	" "	8 " " " " " "
3	Input HP evap.	1 in. from LHS of Input HP
4	"	6 " " " " " "
5	"	11 " " " " " "
6	Input HP adiab.	13 " " " " " "
7	"	13 " " " " " "
8	Coupler section	Left hand end cap
9	" "	Bulkhead
10	" "	Right hand end cap
11	Output HP	24 in. from RHS of Output HP
12	"	24 " " " " " "
13	"	20 " " " " " "
14	"	12 " " " " " "
15	"	4 " " " " " "
16	"	2 " " " " " "
17	Cold plate	
18	Cold plate	

High limit - on heater block close to sensor volume

ENGINEERING SKETCH	TRW SYSTEMS GROUP, ONE SPACE PARK • REDONDO BEACH, CALIFORNIA	
ORIGINATOR: J Ennis	DATE: 10/14/75	VMHP INSTRUMENTATION
MJO		SIZE: A; CODE IDENT NO.: 11982; SK 75061
		SCALE: ; SHEET 1 OF

SYSTEMS 523 REV. 12-71

ORIGINAL PAGE IS
OF POOR QUALITY

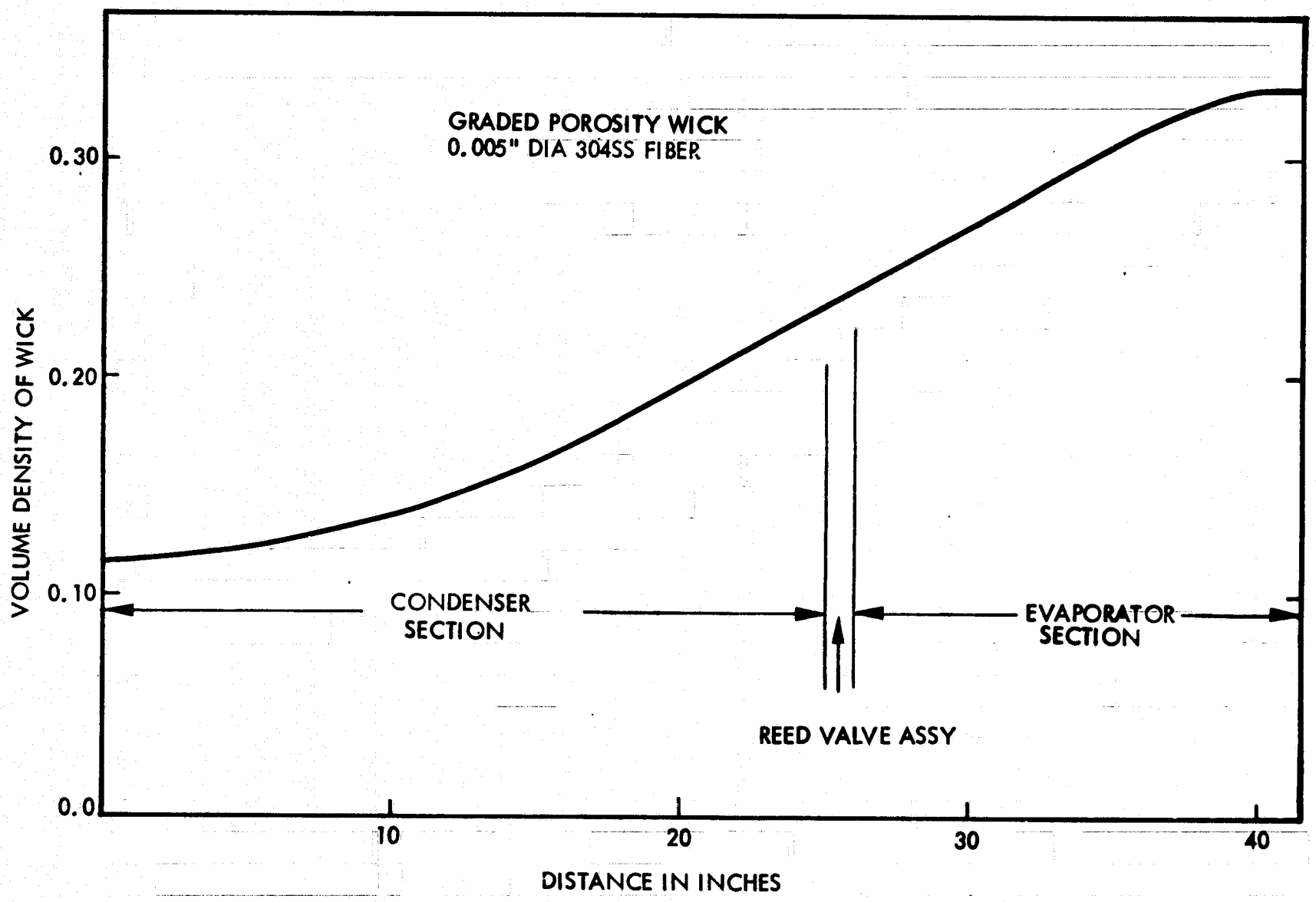

Figure A-1. Heat Pipe Diode Wick Porosity

ORIGINAL PAGE IS
OF POOR QUALITY

APPENDIX B

Listing of computer program VMHP to simulate vapor-modulated Heat Pipe Performance

```
00100       PROGRAM VMHP(INPUT,OUTPUT,TAPE5=INPUT,TAPE6=OUTPUT)
00110       COMMON/ALL/C1,C2,RI,RTS,RG,RW,RS,RV,RO,RE,T1,T2,TE,TB,TV,TI,
00120      1L,LWET,LV,DMEN,D,DD,A,AA,ML,MLSMAL,MLFULL,UG,UW,Q1E,Q12,Q,
00130      2VISV,VISL,RHOL,RHOV,HFG,SIGMA,KTAO,TIME,DT
00140      3,DPV,TSET,UML
00150       REAL L,LWET,LV,ML,MLSMAL,MLFULL,KTAO
00160       N=60
00170       CALL DATA
00180       TIME=-DT
00190  100  DO 101 I=1,N
00200       TIME=TIME+DT
00210       CALL RUNGE(T1,T2,ML,DT)
00220       CALL OUTPUT
00230  101  CONTINUE
00240       STOP
00250       END
00260 C
00270 C     UPDATE T1,T2,ML
00280 C
00290       SUBROUTINE RUNGE(Y10,Y20,Y30,H)
00300       CALL DELTA(Y10,Y20,Y30,DY1,DY2,DY3)
00310       SUM1=DY1
00320       SUM2=DY2
00330       SUM3=DY3
00340       Y1=Y10+DY1*H/2.
00350       Y2=Y20+DY2*H/2.
00360       Y3=Y30+DY3*H/2.
00370       CALL DELTA(Y1,Y2,Y3,DY1,DY2,DY3)
00380       SUM1=SUM1+2.*DY1
00390       SUM2=SUM2+2.*DY2
00400       SUM3=SUM3+2.*DY3
00410       Y1=Y10+DY1*H/2.
00420       Y2=Y20+DY2*H/2.
00430       Y3=Y30+DY3*H/2.
00440       CALL DELTA(Y1,Y2,Y3,DY1,DY2,DY3)
00450       SUM1=SUM1+2.*DY1
00460       SUM2=SUM2+2.*DY2
00470 00480       Y1=Y10+DY1*H
00490       Y2=Y20+DY2*H
00500       Y3=Y30+DY3*H
00510       CALL DELTA(Y1,Y2,Y3,DY1,DY2,DY3)
00520       Y10=Y10+(SUM1+DY1)*H/6.
00530       Y20=Y20+(SUM2+DY2)*H/6.
00540       Y30=Y30+(SUM3+DY3)*H/6.
00550       RETURN
00560       END
00570 C
00580 C     CALCULATE DT1/DT,DT2/DT, AND DML/DT
00590 C
00600       SUBROUTINE DELTA(X1,X2,X3,DT1DT,DT2DT,DMLDT)
00610       COMMON/ALL/C1,C2,RI,RTS,RG,RW,RS,RV,RO,RE,T1,T2,TE,TB,TV,TI,
00620      1L,LWET,LV,DMEN,D,DD,A,AA,ML,MLSMAL,MLFULL,UG,UW,Q1E,Q12,Q,
00630      2VISV,VISL,RHOL,RHOV,HFG,SIGMA,KTAO,TIME,DT
00640      3,DPV,TSET,UML
```

ORIGINAL PAGE IS
OF POOR QUALITY

```
      REAL L,LWET,LV,ML,MLSMAL,MLFULL,KTAO
      T1=X1
      T2=X2
      ML=X3
      CALL RELAX
      DT1DT=(Q-Q1E-Q12)/C1
      DT2DT=Q12/C2
      IF(UML.EQ.0.) GO TO 100
      X=UG/RG+UW/RW
      X=RV+1./X
      EMEVAP=(TI-TB)/X/HFG
      CO1=4.*RHOL/KTAO/VISL
      CO1=CO1*(DD**2*FWET*AA/L+D**2*A/LWET)
      CO2=4.*SIGMA/DMEN
      EMIN=CO1*(CO2-DPV)*4.17E8
      DMLDT=-EMEVAP+EMIN
      RETURN
100   DMLDT=0.
      RETURN
      END
C
C     CALCULATE Q1E,Q12,Q, AND RV
C
      SUBROUTINE RELAX
      COMMON/ALL/C1,C2,RI,RTS,RO,RW,RS,RV,RO,RE,T1,T2,TE,TB,TV,TI,
     1L,LWET,LV,DMEN,D,DD,A,AA,ML,MLSMAL,MLFULL,UG,UW,Q1E,Q12,Q,
     2VISV,VISL,RHOL,RHOV,HFG,SIGMA,KTAO,TIME,DT
     3,DPV,TSET,UML
      REAL L,LWET,LV,ML,MLSMAL,MLFULL,KTAO
      CALL TEST
      Q12=(T1-T2)/RTS
      IF(T2.GE.TSET) GO TO 200
      CO1=2.*RHOV*HFG*AA*DD**2/KTAO/LV/VISV
      TV=TV+5.
      TB=TB-5.
      ICOUNT=0
100   TVOLD=TV
      ICOUNT=ICOUNT+1
      IF(ICOUNT.GT.10)  STOP
      TBOLD=TB
      PVTV=PV(TV)
      PVTB=PV(TB)
      DPV=PVTV-PVTB
50    RV=(TV-TB)/(CO1*DPV*4.17E8)
      RT=UG/RG+UW/RW
      RT=1./RT+RV
      RT=1./RS+1./RT
      RT=1./RT+RI+RO+RE
      Q1E=(T1-TE)/RT
      TB=TE+Q1E*(RE+RO)
      TI=T1-Q1E*RI
      TV=TI-(Q1E-(TI-TB)/RS)/(UW/RW+UG/RG)
      ERTB=ABS(1.-(TB+460.)/(TBOLD+460.))
```

ORIGINAL PAGE IS
OF POOR QUALITY

```
01180        ERTV=ABS(1.-(TV+460.)/(TVOLD+460.))
01190        IF(ERTB.LT..001.AND.ERTV.LT..001) GO TO 101
01200        TB=(TB+TBOLD)/2.
01210        TV=(TV+TVOLD)/2.
01220        GO TO 100
01230   200  RT=UG/RG+UW/RW
01240        RT=RT+1./RS
01250        RT=1./RT+RI+RO+RE
01260        Q1E=(T1-TE)/RT
01270        TB=TE+Q1E*(RE+RO)
01280        TI=T1-Q1E*RI
01290        TV=TI-(Q1E-(TI-TB)/RS)/(UW/RW+UG/RG)
01300   101  RETURN
01310        END
01320 C
01330 C      CALCULATE UG,UW,UML,DMEN,FWET, AND LWET
01340 C
01350        SUBROUTINE TEST
01360        COMMON/ALL/C1,C2,RI,RTS,RG,RW,RS,RV,RO,RE,T1,T2,TE,TB,TV,TI,
01370       1L,LWET,LV,DMEN,D,DD,A,AA,ML,MLSMAL,MLFULL,UG,UW,Q1E,Q12,Q,
01380       2VISV,VISL,RHOL,RHOV,HFG,SIGMA,KTA0,TIME,DT
01390       3,DPV,TSET,UML
01400        REAL L,LWET,LV,ML,MLSMAL,MLFULL,KTA0
01410        UML=1.
01420        IF(ML.EQ.MLFULL) GO TO 100
01430        IF(ML.GT.MLSMAL) GO TO 101
01440        FWET=0.
01450        DMEN=D
01460        UG=0.
01470        UW=ML/MLSMAL
01480        LWET=UW*L
01490        RETURN
01500   101  FWET=(ML-MLSMAL)/(MLFULL-MLSMAL)
01510        LWET=L
01520        DMEN=DD
01530        UG=1.
01540        UW=1.
01550        RETURN
01560   100  IF(T2.GE.TSET) UML=0.
01570        DMEN=DD
01580        FWET=1.
01590        LWET=L
01600        UG=1.
01610        UW=1.
01620        RETURN
01630        END
01640 C
01650 C      CALCULATE VAPOR PRESSURE
01660 C
01670        FUNCTION PV(Z)
01680        DATA A1,A2,A3,A4,A5
01690       1/13.92374,-4.92174,2.065018E-1,-7.579597E-2,0./
01700        X=Z+460.
```

```
01710         X=1000./X
01720         X2=X*X
01730         X3=X2*X
01740         X4=X3*X
01750         Y=A1+A2*X+A3*X2+A4*X3+A5*X4
01760         Y=EXP(Y)
01770         PV=144.*Y
01780         RETURN
01790         END
01800 C
01810 C       PRINT OUTPUT
01820 C
01830         SUBROUTINE OUTPUT
01840         COMMON/ALL/C1,C2,RI,RTS,RG,RW,RS,RV,RO,RE,T1,T2,TE,TB,TV,TI,
01850        1L,LWET,LV,DMEN,D,DD,A,AA,ML,MLSMAL,MLFULL,UG,UW,Q1E,Q12,Q,
01860        2VISV,VISL,RHOL,RHOV,HFG,SIGMA,KTAO,TIME,DT
01870        3,DPV,TSET,UML
01880         REAL L,LWET,LV,ML,MLSMAL,MLFULL,KTAO
01890         IF(TIME.EQ.0.) PRINT1
01900    1    FORMAT(1X,*TIME(SEC)*,6X,*TBLOCK(F)*,6X,*TSENSOR(F)*,
01910        15X,*TVAPOR(F)*)
01920         PRINT 2,TIME,T1,T2,TV
01930    2    FORMAT(1X,4(E11.4,4X))
01940         RETURN
01950         END
01960 C
01970 C       INPUT DATA
01980 C
01990         SUBROUTINE DATA
02000         COMMON/ALL/C1,C2,RI,RTS,RG,RW,RS,RV,RO,RE,T1,T2,TE,TB,TV,TI,
02010        1L,LWET,LV,DMEN,D,DD,A,AA,ML,MLSMAL,MLFULL,UG,UW,Q1E,Q12,Q,
02020        2VISV,VISL,RHOL,RHOV,HFG,SIGMA,KTAO,TIME,DT
02030        3,DPV,TSET,UML
02040         REAL L,LWET,LV,ML,MLSMAL,MLFULL,KTAO
02050         ACCEPT DT,TE
02060         DATA C1,C2,RTS,RI,RS,RW,RG,RO,RE
02070        1/.57,6.00E-3,2.10,4.40E-2,115.,3.E-1,2.20E-2,2.90E-2,2.90E-2/
02080         DATA A,AA,D,DD,L,LV,MLSMAL,MLFULL,KTAO
02090        1/5.35E-4,5.35E-4,6.95E-5,1.39E-4,.5,7.5E-2,1.07E-2,2.14E-2,152./
02100         DATA RHOL,RHOV,SIGMA,VISV,VISL,HFG
02110        1/37.,.705,1.18E-3,2.15E-2,2.83E-1,478./
02120         DATA T1,T2,TSET,Q
02130        1/75.,75.,75.,341./
02140         ML=MLFULL
02150         TV=T1
02160         TB=TE
02170         RETURN
02180         END
```

ORIGINAL PAGE IS
OF POOR QUALITY